HERON is jointly edited by:
STEVIN-LABORATORY of the department of Civil Engineering, Delft University of Technology, Delft, The Netherlands
and
INSTITUTE TNO for Building Materials and Building Structures, Rijswijk (ZH), The Netherlands.
HERON contains contributions based mainly on research work performed in these laboratories on strength of materials, structures and materials science.



*Secretary:*
G. J. van Alphen
Stevinweg 1
P.O. Box 5048
2600 GA Delft, The Netherlands
Tel. 0031-15-785919
Telex 38070 BITHD

HERON vol. 27 1982 no. 3

**Contents**

# CONCRETE UNDER IMPACT LOADING TENSILE STRENGTH AND BOND

*H. W. Reinhardt*

Delft University of Technology
Department of Civil Engineering
Stevin Laboratory
Stevinweg 4, P.O. Box 5048, 2600 GA Delft, The Netherlands

**Abstract** ..... 2
**Foreword** ..... 3
**1 Introduction** ..... 5
**2 Study of the literature** ..... 6
2.1 Loading rates associated with impact loads 6
2.2 Suitable methods of testing ..... 6
2.3 Effect of loading rate on tensile strength and stress-strain diagram of concrete .... 7
2.4 Effect of loading rate on bond between steel and concrete ..... 8
2.5 Effect of repeated impact loading on tensile strength of concrete ..... 9
2.6 Theories to explain the various influences 9
2.7 Conclusion ..... 9
**3 Experimental research** ..... 10
3.1 Method of investigation ..... 10
3.2 Research program ..... 13
3.2.1 Once-only impact tensile loading ..... 13
3.2.2 Repeated impact tensile loading ..... 14
3.2.3 Bond tests ..... 14
**4 Results** ..... 15
4.1 Once-only impact tensile loading ..... 15
4.2 Repeated impact tensile loading ..... 19
4.3 Bond tests ..... 22
4.3.1 General ..... 22
4.3.2 Force-displacement relations ..... 23
4.3.3 Processing the results for ribbed steel ... 28
4.3.4 Translating the results into the behaviour for long bond lengths ..... 30

CUR VB

*This publication has been issued in close co-operation with the Netherlands Committee for Research, Codes and Specifications for Concrete (CUR-VB).*

**5 Comparison with codes and standards** ..... 31
5.1 Calculation of tensile strength from cube (compressive) strength ..... 31
5.2 Repeated impact tensile loading ..... 35
5.3 Bond ..... 36
**6 Summary and conclusions** ..... 37
**7 Notations** ..... 40
**8 References** ..... 41
**Appendix** ..... 43

Publications in HERON since 1970

**Abstract**

Uniaxial impact tensile tests on plain concrete were carried out with the aid of Split Hopkinson Bar equipment with stress rates of up to 60 000 $N/mm^2 \cdot s$. Various concrete mixes were investigated under dry and wet conditions. All the concretes showed an increase in strength with increasing stress rate. At very high stress rates the strength may attain twice the static tensile strength.

Repeated impact tensile loading reduces the strength considerably more than cyclic loading does with conventional stress rates.

The bond between reinforcing steel and concrete was studied in pull-out tests with short embedment length. The results showed the bond strength and stiffness of deformed bars to increase with the loading rate, whereas plain bars and prestressing strands were hardly affected by the loading rate.

It proved possible to formulate the tensile strength and the bond behaviour as a function of stress rate by means of a power function. Relations between compressive strength and tensile strength are given for various stress rates.

**Key words**

Concrete, tensile strength, bond strength, impact loading, impact fatigue, testing methods.

## CONCRETE UNDER IMPACT LOADING. TENSILE STRENGTH AND BOND

### Foreword

In recent years, exceptional loads on structures, such as impact loads, have claimed an increasing amount of attention. This is bound up with the introduction of new types of structure and with safety aspects, which received rather less attention in the past.

Despite the fact that offshore platforms, nuclear power stations and storage tanks have been constructed of concrete, there are today still gaps in our knowledge of the behaviour of this material at high rates of loading. The same applies to the reinforcement of concrete foundation piles, the design of which can be placed on a really sound basis only if the properties of the concrete and the bond between steel and concrete when subjected to high loading rates are known.

The lack of adequate knowledge of these matters associated with material behaviour prompted the CUR-VB to set up Committee C 35 "Concrete under impact loading" in 1976.

On completion of its research the Committee was constituted as follows:
Ir. J. Schippers, Chairman
Ir. J. J. Eberwijn, Secretary
Ir. W. Haitsma
Ir. J. J. de Heer
Ir. J. van Keulen
Prof. Dr.-Ing. H. W. Reinhardt
Ir. A. B. M. van der Plas, Mentor

Ir. W. H. M. van Lange participated in the Committee's work since its inception. He was succeeded by Ir. J. van Keulen in 1979.

The research was carried out in the Stevin Laboratory of the Delft University of Technology. Ir. H. A. Körmeling, Prof. Dr.-Ing. H. W. Reinhardt, Ir. E. Vos, Ir. A. W. de Vries and Dipl.-Ing. A. J. Zielinski were associated with these investigations.

Financial support has been provided by Stichting CUR-VB, Stichting Bouwresearch, Betonson B.V., Haitsma Bouwindustrie (HBI) B.V., PIT Beton Heipalenfabriek Kamperland B.V., Charcon Ringvaart B.V., Schokindustrie B.V., Voorbij's Beton B.V. and IJsselmeer Beton B.V. This is gratefully acknowledged.

The present issue of "Heron" is based on CUR-VB Report No. 106 entitled "Concrete under impact loading - tensile strength and bond".

# Concrete under impact loading
# Tensile strength and bond

## 1 Introduction

Impact load acting on concrete structures or parts thereof is of common occurrence. Examples that come to mind are: collision of vehicles or vessels with bridge piers or superstructures, collisions with offshore structures, aircraft crashes, explosions in or near structures, and the effect of explosions of bombs or projectiles. Apart from these exceptional loads, structures may also be subjected to functional impact loads, notably exemplified by those acting on piles during the driving operation. These loads differ from ordinary static loads in the very much shorter duration of loading, which in the case of impact is measured in milliseconds or at most in seconds.

If the designer wishes to take account of impact loads, he will have to know whether the properties of the materials - such as compressive strength, tensile strength, stress-strain behaviour, bond between steel and concrete - are perhaps altered under the influence of the rate of loading. If these properties were found to be impaired as a result of high loading rates, it would mean that the safety based on the static structural properties would be reduced under impact loading. Conversely, if the properties were found to become better under impact loading, it would be possible to design structures more economically to meet those conditions and yet fulfil the safety requirements.

Questions such as these relating to material behaviour led to the setting up of CUR-VB Committee C 35 "Concrete under impact loading". This Committee's task was limited to the investigation of three important mechanical properties, namely, the tensile strength of concrete, the stress-strain diagram of concrete in tension, and the bond between steel and concrete. These three properties play an essential part in connection with the cracking of reinforced concrete or prestressed concrete piles during driving. But in all the other above-mentioned types of impact loading these properties have a share in determining the degree and extent of cracking, crack width and crack spacing. Furthermore, these properties significantly affect structural loadbearing capacity under conditions of punching shear or bending shear. Tensile strength is also a parameter associated with the formulation of the biaxial and triaxial strength of concrete.

In most cases the behaviour of concrete under once-only impact loading will more particularly be of importance.

In pile-driving, however, there is repeated impact loading. The number of impact load applications will vary, depending on the length of the pile and on soil conditions, but will usually not exceed 3000. Moreover, the wish to apply the results to piles was what prompted the investigation of the effect of repeated loading on the tensile strength of concrete.

Also, the present investigators' own results were compared with the information given in foreign codes of practice.

The development of a testing method was an important feature of the investigation as a whole, and a full description of this has accordingly been included in the report.

Finally, on the basis of the research results obtained, recommendations for practical use are offered.

## 2 Study of the literature

Before the actual research was started, a study of the available literature was undertaken with regard to the following points:

- loading rates associated with impact loads;
- suitable methods of testing;
- effect of loading rate on the tensile strength and stress-strain diagram of concrete;
- effect of loading rate on the bond between steel and concrete;
- effect of repeated impact loading on the tensile strength of concrete;
- theories to explain the various influences.

These points will now be briefly examined.

### 2.1 *Loading rates associated with impact loads*

The loading rates (increase in stress per unit time) for various cases are given in Table 1. Of course, these figures are very approximate and subject to considerable scatter, because the mass and stiffness of the structure itself determine the rate of loading that occurs at a section. The order of magnitude of the associated strain rate is also indicated in the table.

Table 1. Loading rates associated with various cases of loading

| loading case | loading rate $\dot{\sigma}$ ($N/mm^2 \cdot ms$) | strain rate $\dot{\varepsilon}$ (1/s) |
|---|---|---|
| collision with vessel | $10^{-4}$ to $10^{-3}$ | $10^{-5}$ |
| collision with vehicle | $10^{-3}$ to $10^{-2}$ | $10^{-4}$ |
| gas explosion | $10^{-3}$ to $10^{-2}$ | $10^{-4}$ |
| crashing aircraft | $10^{-1}$ to $10^{0}$ | $10^{-2}$ |
| earthquake | $5 \cdot 10^{-1}$ to $10^{2}$ | $10^{-2}$ to $3 \cdot 10^{0}$ |
| pile-driving | $10^{0}$ to $3 \cdot 10^{1}$ | $3 \cdot 10^{-2}$ to $10^{0}$ |

The highest loading rates are in the region of 100 $N/mm^2 \cdot ms$ and occur in earthquakes. In pile-driving the (tensile) loading rates are between 1 and 30 $N/mm^2 \cdot ms$. The maximum strain rates are approximately 3/s (= 300%/s).

### 2.2 *Suitable methods of testing*

Three methods are commonly employed for the testing of tensile strength, namely, the flexural test, the splitting test and the direct (or axial) tensile test. From the point of view of execution, the flexural and the splitting test are much simpler than the direct

tensile test, but their disadvantages are that the stress distribution in the test specimen cannot be measured and that the strains and strain rates in the specimen are not constant. The known stress distributions are based on linear elastic theory, which is valid only for low stresses in concrete. On the other hand, the direct tensile test with its axially central load application gives a well-defined relation between tensile force and stress, while the strains and strain rates or stress rates are constant over the cross-section of the specimen. The literature gives no information on how a direct tensile test can be performed at high loading rates.

The bond between steel and concrete can be determined in various ways, depending on the purpose of the investigation. If a local relation between force and displacement has to be determined, as is needed for calculating the bond stresses along a reinforcing bar, a pull-out test with a short bond length is a suitable method. The effect of the loading rate can be investigated by pulling an embedded bar out of the concrete at different rates (speeds of pull-out) and measuring the force needed for this.

### 2.3 *Effect of loading rate on tensile strength and stress-strain diagram of concrete*

The effect that the rate of loading has upon the tensile strength of concrete has been dealt with in a small number of publications [1 to 5], the results of which are shown in Fig. 1. Evidently the direct tensile strenght increases as the loading rate is higher.

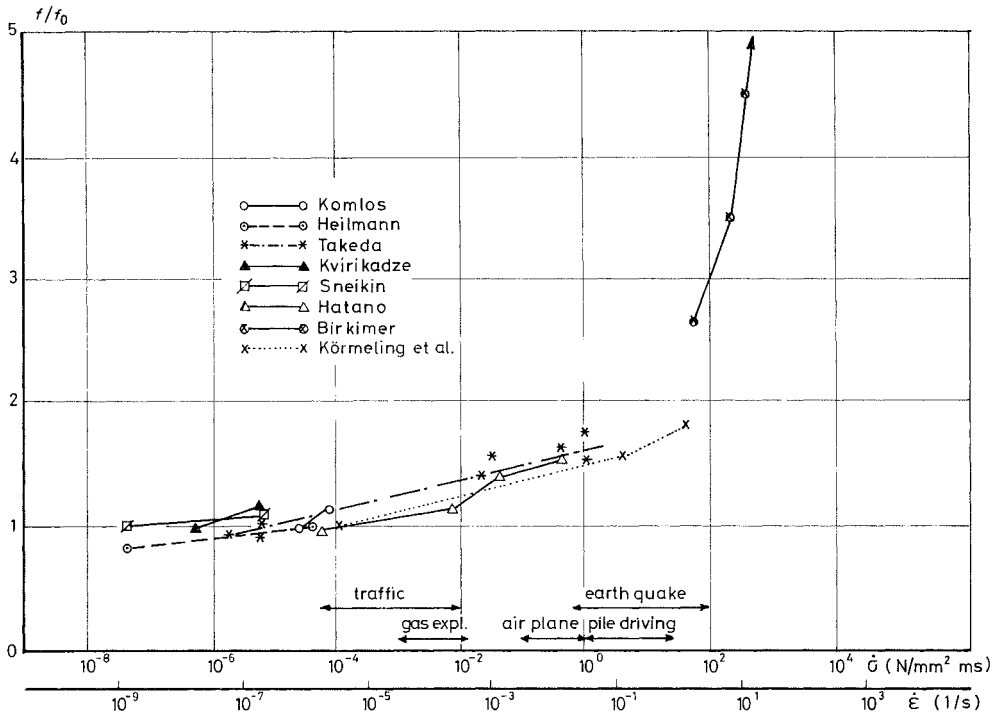


Fig. 1. Relative impact tensile strength as a function of loading rate.

It is to be noted that most of the tests were performed at rates of less than 1 $N/mm^2 \cdot ms$ and that only one investigation involving very high rates has been reported in the literature. The range between 1 $N/mm^2 \cdot ms < \dot{\sigma} < 100\ N/mm^2 \cdot ms$, which is more particularly of interest in connection with the behaviour of piles, was not investigated.

With regard to the effect of the loading rate on the stress-strain diagram there is lack of agreement between the conclusions of the various investigators. They concur only on the fact that the modulus of elasticity increases with higher loading rates. On the subject of ultimate strain opinions are divided. Some investigators assert that it decreases with higher loading rates – i.e., the material displays a more brittle type of behaviour – whereas others conclude that the ultimate strain, like the strength, increases with higher rates.

### 2.4 *Effect of loading rate on bond between steel and concrete*

Only two reports of researches concerned with the effect of loading rate on steel-to-concrete bond were found [6, 7]. In pull-out tests on ribbed bars with a short bond length of 112 mm the maximum bond stress was found to increase with the loading rate (see Fig. 2). Although this trend appears reasonable, a correct interpretation of the results is

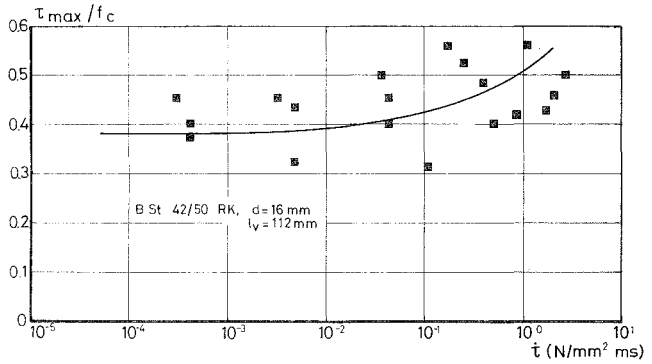


Fig. 2. Effect of loading rate on pull-out resistance of ribbed reinforcing steel [6].

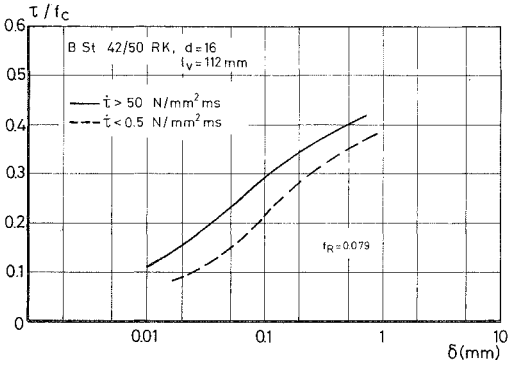


Fig. 3. Relation between bond stress and pull-out at two pull-out rates [6].

rendered difficult by the considerable scatter they exhibit. As can be deduced from Fig. 3, for a particular bond stress the pull-out becomes less according as the rate increases. The same trend emerges from the results of the other research [7], from which it was inferred that at pull-out rates corresponding to a time of 10 ms the bond strength approaches the uniaxial cylinder compressive strength.

### 2.5 *Effect of repeated impact loading on tensile strength of concrete*

No information on the effect of impact load repetition on concrete could be obtained from the literature. For the sake of completeness, however, it is to be noted that a comprehensive report on compressive impact loading on concrete appeared fairly recently in Sweden [8].

### 2.6 *Theories to explain the various influences*

From the study of the literature it emerged that some mechanical properties of concrete at high loading rates have indeed been experimentally investigated, but that no systematic research on the effect of various parameters has been carried out. Hence it would be of real value to have a theory or model to account for the phenomena in question. Mihashi and Izumi [9] developed a theory based on fracture mechanics and presupposing that there exists a particular failure probability per unit of time. Subject to these conditions a generally-valid relation between loading rate and strength is derived:

$$\frac{f}{f_0} = \left(\frac{\dot{\sigma}}{\dot{\sigma}_0}\right)^{\frac{1}{1+\beta}} \tag{1}$$

where $\beta$ is a material parameter that depends on the composition of the concrete, on the temperature and on the climatological conditions. An extension of this theory to repeated loading [10] gives a logarithmic relation between fatigue strength and the number of load repetitions. This theory is suitable for indicating the effect of the loading, but it cannot predict the effect of the type of concrete, the temperature, the humidity, etc. To determine these things requires experimental investigations.

For bond there exists as yet no physical model, apart from elastic analyses and numerical treatments of the problem with the help of finite element programs. On the basis of the theory of Mihashi and Izumi [9] and the assumption that the strength of the concrete substantially governs the bond behaviour, it can be presumed that a relation as expressed by (1) exists also for bond.

### 2.7 *Conclusion*

The conclusion drawn from the study of the literature was that as yet relatively little was known about the behaviour of concrete under impact loading and that systematic research would therefore be very useful.

## 3 Experimental research

### 3.1 *Method of investigation*

As Table 1 shows, the loading rates that may occur in pile-driving or in earthquakes are of the order of 10 to 30 $N/mm^2 \cdot ms$. In relation to a static tensile test, which is performed at an average loading of 0.05 $N/mm^2 \cdot s$, these impact rates are thus higher by a factor ranging from 200 000 to 600 000. Such rates were not attainable with the hydraulic testing equipment available in the Stevin Laboratory of the Delft University of Technology. For this reason a new method of testing was sought.

In the end, a method based on the "Split Hopkins Bar" principle was chosen [11]. This principle was developed as follows:

In a long bar of elastic material a tension wave is generated, which is transmitted into a test specimen and which then continues into a second elastic bar, after which the tension wave is damped out.

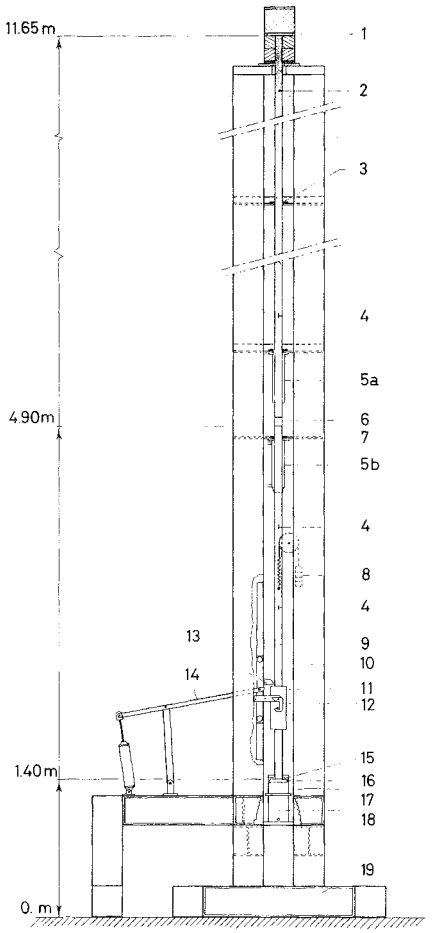


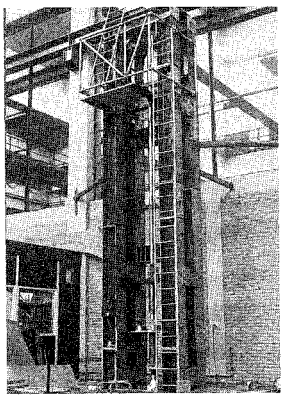

1 buffer
2 upper bar
3 guide
4 strain gauge
5a upper cooling jacket
5b lower cooling jacket
6 concrete test specimen ø 74 x 100 mm
7 working platform
8 counterweight
9 lower bar
10 frame
11 drop weight
12 coupling
13 uncoupling
14 lifting device
15 demping material
16 anvil
17 guide tube
18 pneumatic jack
19 frame base

Fig. 4. Schematic diagram and photograph of test set-up.

The loading arrangement is shown schematically in Fig. 4. The drop-weight 11 slides along the lower bar (aluminium, 74 mm diameter) and strikes the thickened end (anvil) of this bar, so that a tension wave is set up in the latter.

The maximum stress of the wave is determined by the height of fall of the weight, the magnitude of the weight, and the contact between the weight and the anvil. Greater height of fall, greater weight and hard contact produce high stresses. The loading rates and the wavelength are mainly governed by the contact between the drop-weight and the anvil. In order to obtain a lower rate of loading, a soft material (cardboard, rubber) is used for the interposed layers. In this way rates ranging from 2 to 60 $N/mm^2 \cdot ms$ can be obtained. As appears from Fig. 4, the tension wave is introduced into the lower bar and then passes through the test specimen, which is glued with polyester resin between the two bars. If the mechanical impedances of the specimen and the bars are equal, the wave will pass undisturbed. But if the impedances differ, the wave will be partially reflected. With normal concrete between aluminium bars the reflected proportion is 5 to 20%, while 80 to 95% passes. It is this passing proportion that loads the test specimen.

If the strain in the upper bar is measured, the average stress in the specimen can be calculated from the condition that the same force must act at the top of the specimen and at the underside of the upper bar. No. 4 in Fig. 4 denotes a measuring position. The strain of the specimen is measured either by proximity transducers (VRPT) or by glued-on electric resistance strain gauges. When these two measurements have been synchronized - the wave first passes through the specimen and only then reaches measuring position 4 - the stress-strain ($\sigma$-$\varepsilon$) diagram of the concrete can be plotted.

The dimensions of the test rig have been so chosen that concrete with a maximum aggregate particle diameter of 16 mm can be properly tested (74 mm diameter bars) and that even at low rates of loading (2 $N/mm^2 \cdot ms$) the reflections from the ends of the bars do not reach the specimen before the wave on its initial journey has passed the specimen. This testing arrangement was employed both for the impact loading tests on concrete and for the bond tests.

The mechanism which, for repeated impact loading, raised and released the drop-weight 16 times a minute is shown in Fig. 4 (Nos. 13, 14). The number of load applications up to failure was recorded.

The impact tensile tests on plain (unreinforced) concrete were performed on cylinders, 74 mm in diameter and 100 mm in height, which had been drilled from a block of concrete. The bond between steel and concrete was tested on pull-out specimens with a short bond length. Because of the hoop tensile forces due to the bond it was necessary to employ a concrete cylinder of 102 mm diameter instead of 74 mm. The length of the cylinder was 130 mm, and the bond length of the 10 mm diameter reinforcing bars, and of the 9.6 mm diameter prestressing strands, was 30 mm.

Fig. 5 is a drawing which shows the test specimen glued to the aluminium bars - with the aid of an adapter unit at the top and a steel plate underneath. The displacement of the bar is measured in a recess in the adapter against the end of the bar with the aid of a proximity transducer (VRPT). The force in the bar is determined with electric resis-

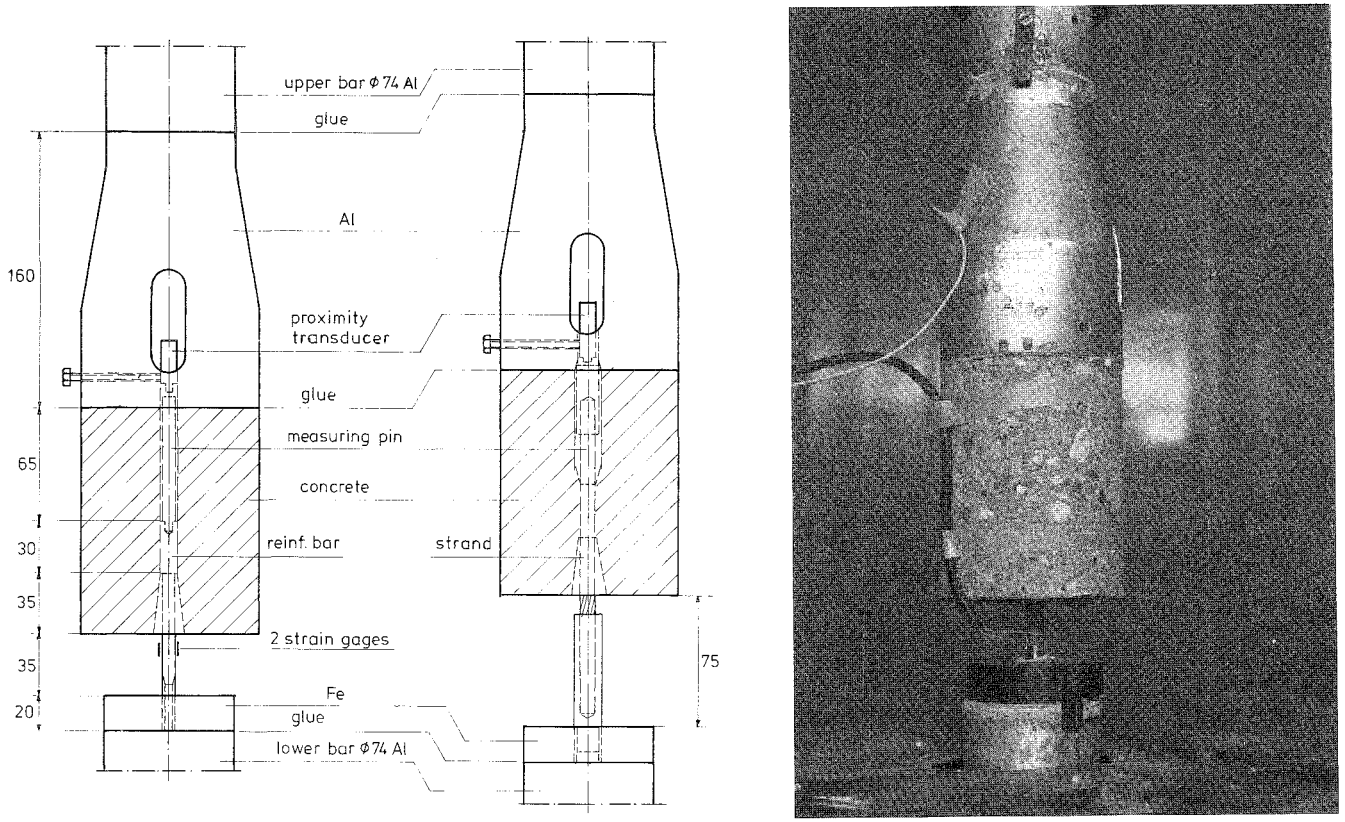


Fig. 5. Pull-out test specimens.

tance strain gauges. In this way the relation between the pull-out force and the displacement of the steel relatively to the concrete at any particular time is established.

The results of the measurements were recorded with a transient recorder (Nicolet, Explorer II), with a measuring frequency of 2 MHz and a 4 k memory, and processed by means of the HP 21 MX laboratory computer.

Static reference tests were performed on a hydraulic testing machine. These tests were concerned with determining the static tensile strength of the concrete used.

## 3.2 *Research program*

### 3.2.1 Once-only impact tensile loading

On the basis of the preliminary study it was decided to apply loading rates varying between 3 and 30 $N/mm^2 \cdot ms$. The effect of the following parameters on the impact tensile strength was investigated:

- type of cement;
- cement content;
- water-cement ratio;
- maximum aggregate particle size;
- moisture content of the concrete;
- direction of loading in relation to the direction of casting of the specimen.

The type of aggregate was kept unchanged (rounded particles, grading curve as in Table A1 of Appendix A).

The age of the concrete at the time of testing was about 28 days, and the temperature about 20° C.

In a preliminary program the parameters listed in Table 2 were investigated.

Table 2. Parameters investigated in the preliminary program

| | |
|---|---|
| loading rate | 3 and 30 $N/mm^2 \cdot ms$ |
| type of cement | portland cement A, B and C<br>portland blastfurnace cement A and B |
| cement content | 300, 325 en 375 $kg/m^3$ |
| water-cement ratio | 0,40 en 0,45 |
| max. aggregate size | 8, 16 and 24 mm |

The results of these investigations showed that the cement type was of minimal influence, that the water-cement ratio should be studied within a wider range of values, and that an aggregate particles size in excess of 16 mm resulted in too much scatter because of the relation between such size and the test specimen diameter of 74 mm.

The parameters for the main program were chosen as listed in Table 3. The cement employed was portland cement of class B, and the maximum aggregate particle size was 16 mm.

Table 3. Parameters investigated in the main program

| | |
|---|---|
| loading rate | 3 and 30 $N/mm^2 \cdot ms$ |
| cement content | 325 and 375 $kg/m^3$ |
| water-cement ratio | 0.40 and 0.50 |
| moisture condition of the concrete | dry, wet |
| direction of loading | parallel and perpendicular to the direction of concreting |

The moisture condition designated as "dry" means that the test specimens were stored wet for 14 days and then at 50% relative humidity; "wet" means that they were stored in a humidity chamber up to the time of testing. All the specimens were, on the 14th day, obtained by drilling them out of 200 mm cubes (preliminary program) or out of 300 mm × 600 mm × 250 mm blocks (main program). They were then finished by sawing, to that their end faces were parallel and perpendicular to the longitudinal axis. The results of the accompanying control tests on the concrete mixes are given in Tables A2 and A3 of Appendix A.

### 3.2.2 Repeated impact tensile loading

The parameters for repeated loading were identical with those of the main program with once-only loading, with one exception.

The loading rate was lower, being 2 to 6 $N/mm^2 \cdot ms$, with an average of 5 $N/mm^2 \cdot ms$. The number of load applications up to failure was chosen between 1 and 1000, this latter number being regarded as a target, as is usual in fatigue testing. The results of the control tests are given in Table A3 of Appendix A.

### 3.2.3 Bond tests

In these tests, too, the principal parameter is the loading rate expressed as an increase in bond stress with time. For this purpose four ranges of loading rate were chosen, namely, 100 to 160 $N/mm^2 \cdot ms$, 20 to 40 $N/mm^2 \cdot ms$, approx. 0.08 $N/mm^2 \cdot ms$ and $0.3 \times 10^{-3}$ $N/mm^2 \cdot ms$.

The bond stress is defined as the pull-out force divided by the circumference times the bond length (average bond stress).

The lowest rate can be regarded as constituting static load. As the effect of the loading rate was expected to differ for different types of steel, three types of steel were investi-

Table 4. Steels used in the pull-out tests

| type of steel | yield point or 0.1% proof stress ($N/mm^2$) | modulus of elasticity ($kN/mm^2$) |
|---|---|---|
| plain, ø 10 mm | 285 | 207 |
| ribbed (Hi-bond), ø 10 mm, relative rib area 0.076 | 445 | 212 |
| prestressing strand ø 9,6 mm | 1730 | 200 |

gated, namely, plain and deformed (ribbed) reinforcing bars and strand prestressing tendons.

The mechanical properties of the steels employed are listed in Table 4.
The bond behaviour was investigated for three grades of concrete with average cube strengths of 22, 45 and 55 N/mm$^2$ respectively. The cement employed was portland cement class B, and the maximum aggregate particle size was 16 mm.

The overall review of the pull-out testing program is presented in Table 5. It is to be noted that the tests indicated in the first two columns were performed with the testing technique described (see 3.1), whereas the slow tests were performed on an electro-hydraulic testing machine.

Table 5. Pull-out testing program

| concrete compressive strength $f_{cm}$ (N/mm$^2$) | bond stress rate (N/mm$^2$ · ms) | | | |
|---|---|---|---|---|
| | 100–160 | 20–40 | 0.08 | 0.3 $10^{-3}$ |
| 22 | ribbed | ribbed | ribbed | ribbed |
| 45 | ribbed | ribbed<br>plain | ribbed | ribbed<br>plain |
| 55 | ribbed | ribbed<br>plain<br>strand | ribbed | ribbed<br>plain<br>strand |

## 4 Results

### 4.1 *Once-only impact tensile loading*

All values of the *tensile strength* at high rates of loading are greater than those obtained under static loading. This is the general result of the investigations and is in agreement with the theory (see formula (1)). How much greater the impact tensile strength is than the static tensile strength will depend on the composition of the concrete and on the loading rate. The results will be discussed in this chapter, with reference to a double logarithmic relation of the following form:

$$\ln f = A + B \ln \dot{\sigma} \tag{2}$$

where $f$ is the tensile strength at the loading rate $\dot{\sigma}$ and $A$ and $B$ are coefficients. Formula (2) was chosen because of the ease of computer processing it offers and is identical with formula (1), putting $B = (1+\beta)^{-1}$ and $A = \ln f_0 - (1+\beta)^{-1}$, while $f_0$ and $\dot{\sigma}_0$ are the tensile strength and the loading rate in the static test.

All the results were statistically analysed with a view to verifying the reliability of formula (2). The correlation coefficient and the 95% confidence interval were calculated. The results of the statistical analysis are given separately in Table A4 of Appendix A. Some of the static tests were splitting tests and some were direct (axial) tensile tests. From comparison tests it emerged that the splitting tensile strength is a few per cent higher than the direct tensile strength. This difference is neglected here, however.

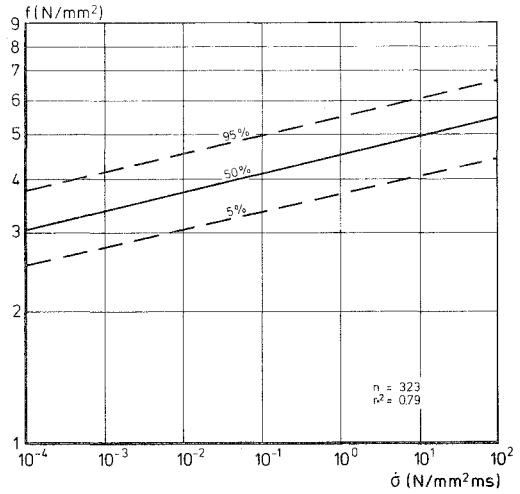


Fig. 6. Relation between tensile strength and loading rate.

Before the various influence parameters are discussed, the results of all the static and impact loading tests will be treated as though they belonged to one statistical population. The regression analysis of the 323 results yields the relation between tensile strength and loading rate, as has been plotted in Fig. 6. The mean tensile strength for static testing ($\dot{\sigma} = 10^{-4}$ N/mm$^2$ · ms) is 3.05 N/mm$^2$, and for impact testing ($\dot{\sigma} = 10^2$ N/mm$^2$) it is 5.50 N/mm$^2$.

From the same calculation are also obtained the bounds between which 90% of all the anticipated results should be situated. These bounds are indicated by dash lines. From Fig. 6 it is also apparent that, in view of the scatter of the results and the slope of the lines, a distinct increase in tensile strength will be achieved only as a result of a substantial increase in loading rate.

A somewhat more general interpretation of the results can be obtained by plotting the relative strength - i.e., the ratio between the strength at a particular loading rate and the static strength - against the ratio of the associated loading rates.
In Fig. 7 the values on the horizontal axis begin with 1 (unity), corresponding to the static test. With increasing rate the strength also increases and attains at $10^6$ a mean value of 1.80 times the static strength. The value which 5% of the results will fail to reach is 1.35, and the value which will be exceeded by 5% of the results is 2.37. From Fig. 7 it also emerges that for a loading rate ratio of $10^3$ the 5% lower limit just coincides with unity. Furthermore, it can be shown statistically that in only 0.05% of the cases there will be no increase in strength at all if the loading rate ratio is increased to $10^6$. The general conclusion is, accordingly, that even at high loading rates there will almost certainly be an increase in tensile strength.

To follow this approximate general interpretation, the various test parameters will now be separately examined. It should be noted from the outset, however, that all of these have much less effect on the result than the loading rate has.

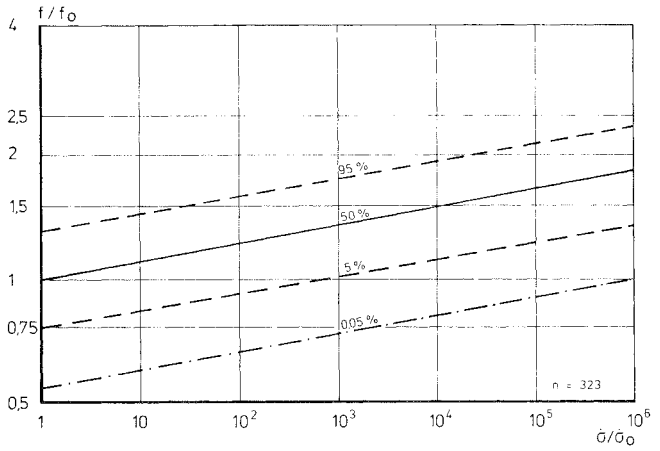


Fig. 7. Relative strength as a function of relative loading rate.

In this research the *maximum aggregate particle size* ranged from 8 mm to 24 mm. From the results it emerged, too, that a larger particle size resulted in a lower impact tensile strength, but bearing in mind that the scatter of the results increased. As regards the *water-cement ratio*, a decrease in this ratio tends to be associated with an increase in impact tensile strength, but then on the other hand the ratio between the impact tensile strength and the static tensile strength decreases. The *cement content* is found to have relatively little effect on the results, though these do indicate that the impact tensile strength increases if the cement content is higher. There was no discernible effect of the *type of cement*, nor of the *moisture condition* of the concrete, upon the impact tensile strength. On the other hand, the effect of the *direction of loading* is very considerable. In tests performed in the direction perpendicular to the direction of casting the impact tensile strength is 20% higher than in tests parallel to the direction of casting the concrete. It was attempted to establish a clear relation between the *cube (compressive) strength* and the impact tensile strength, but without success. Evidently the parameters determining the static compressive strength do not similarly affect the impact tensile strength.

The *stress-strain diagram* ($\sigma$-$\varepsilon$ diagram) of the concrete was determined under static tensile loading and also in the impact tensile test. The average diagram based on four static and twelve impact tests is shown in Fig. 8. It is notable that the modulus of elasticity and the ultimate strain in impact loading tests are larger than in static loading tests. While the static modulus of elasticity (secant modulus determined at the origin of the diagram) was 25 500 N/mm$^2$ at $\sigma = 2$ N/mm$^2$, in the impact test it was 39 500 N/mm$^2$ at the same level of stress. At $\sigma = 5$ N/mm$^2$ this latter value had decreased to 30 000 N/mm$^2$. The strain associated with the highest stress is 0.014% in the static test and 0.024% in the impact test. These results therefore show that concrete behaves in a more rigid, but not in a more brittle manner when subjected to impact loading.

If the underlying factors governing the results of the tests with once-only impact loading are to be elucidated, it will be necessary to consider the composition and struc-

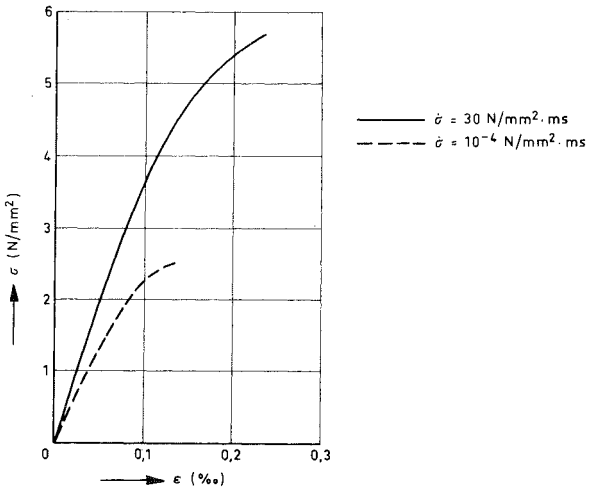


Fig. 8. Stress-strain diagrams for static loading and impact loading.

ture of the concrete in general. Concrete is a composite material consisting of a matrix (hardened cement paste + fine particles) with coarser particles embedded in it. The strength of the matrix and particles, the bond between matrix and particles, and the mix proportions are what determine the behaviour of this composite material. Besides, concrete always contains microcracks, chiefly at the interfaces (boundary surfaces) of the matrix and the particles embedded in it [12].

Having regard to this structure it can reasonably be supposed that these cracks grow during loading and that failure occurs as soon as they exceed a certain length. The question is how the loading rate can affect crack growth. For cracks to grow in size a certain time is required, which is available in static loading tests and even more so in creep tests. Under such circumstances the cracks will extend to zones where the tensile strength or the bond strength is lowest. For this reason the long-term (sustained load) strength is lower than the short-term static strength.

In the case of impact loading, where failure takes place within a few milliseconds, the cracks do not always have an opportunity to seek the zones of least resistance and may therefore instead make their way into higher-strength zones. Also, with cracks extending very rapidly branching of the crack tip may occur [12]. Both aspects demand more energy; hence the measured tensile must be higher as the rate of loading is increased.

The effect of the loading rate diminishes with decreasing difference in mechanical behaviour between the matrix and the particles, e.g., if the water-cement ratio is low. The ratio between impact tensile strength and static tensile strength accordingly decreases from 1.60 for mix 25 (water-cement ratio 0.50) to 1.50 for mix 23 (water-cement ratio 0.40). A similar effect should occur in concrete with a low cement content, because the influence exercised by the hardened cement paste itself becomes less. In concrete containing large aggregate particles there often occur cavities due to water segregation

under these particles, so that their bond to the matrix is poor. The probability of a crack forming under the particles and extending from particle to particle is greater according as the particles are larger, so that the effect of the loading rate diminishes. Conversely, with small aggregate particles the cracks are often compelled to intersect the particles, which requires more energy. The same aspect manifests itself in comparing the results of tests in which the direction of loading is parallel to, or perpendicular to, the direction of casting. In the former case, i.e., where loading direction and casting direction coincide, the cracks tend easily to pass round the particles, whereas with loading perpendicular to the casting direction the cracks are often compelled to intersect the particles. Fracture surfaces of test specimens consistently reveal this difference in behaviour.

The stress-strain diagram calls for some further comment. Differences in stiffness in the initial stages of loading, where crack propagation still plays only a subordinate part, must be sought in the response of the visco-elastic hardened cement paste. As soon as cracking dominates, the arguments presented with regard to the strength now equally apply with regard to the stiffness behaviour: there is greater resistance to deformation and therefore greater stiffness. All the same, the ultimate strain for impact loading is greater than for static loading. This is due to the fact that with impact a crack does not get an opportunity to find the easiest path so as to cause the specimen to fail at its weakest section. Instead, cracks will begin to develop in various sections, with the result that the average ultimate strain over the length of the specimen becomes greater. An indication of the correctness of this argument was obtained at very high loading rates, at which some specimens underwent simultaneous failure at two sections.

### 4.2 *Repeated impact tensile loading*

Repeated impact tensile loading can be regarded as a fatigue test, with constant amplitude, in which the load cycles to failure correspond to a number of impact load applications to failure. The designation "impact fatigue" would appear most appropriate. From fatigue tests it is known that the relation between the maximum stress and the associated number of load applications to failure is a simple function of the following form:

$$\sigma_{max} = A_1 + B_1 \ln N \tag{3}$$

where $A_1$ and $B_1$ are constants which depend on the material and on the test conditions. Now if the maximum stress is referred to the static tensile strength, formula (3) can be written as follows:

$$\frac{\sigma_{max}}{f_0} = A_2 + B_2 \ln N \tag{4}$$

where $A_2$ and $B_2$ likewise are constants.

All the test results have been subjected to a regression analysis with the formulae (3) and (4), the results of which are contained in Table A5 and A6 of Appendix A.

An example of a particular concrete mix composition (mix 23) is presented in Fig. 9,

where the mean regression line and the 2.5% and 97.5% bounds have been plotted. The decrease in the number of load applications to failure with increasing maximum stress is clearly manifest.

The results of 89 repeated impact tests (impact fatigue tests) are embodied in Figs. 10 and 11, not taking account of the different mix compositions. From Fig. 10 it emerges that the mean absolute value of 4.3 N/mm$^2$ found in once-only loading decreases to 2.0 N/mm$^2$ for 1000 load applications. According to this relation the absolute value will decrease to zero for 750 000 load applications. It is very unlikely, however, that this will indeed occur, and therefore the validity of thus extrapolating outside the range actually covered by testing must be called in question. Further tests with a low loading level would have to be performed in order to obtain more certainty in the matter.

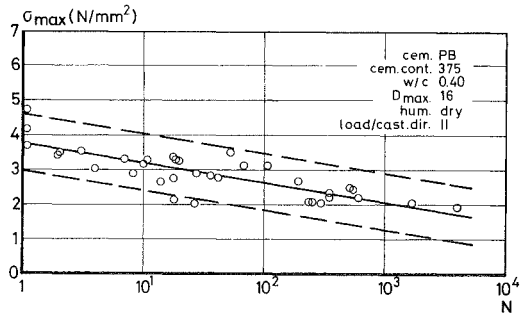


Fig. 9. Relation between maximum stress and the number of impact loads to failure for a particular concrete composition.

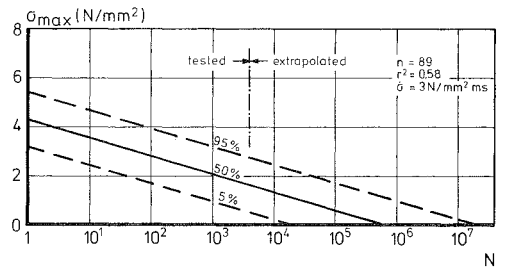


Fig. 10. Relation between maximum stress and the number of impact loads for all the results.

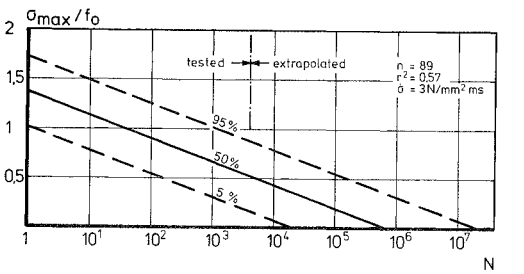


Fig. 11. Relation between relative maximum stress and the number of impact loads for all the results.

In Fig. 11 the relative maximum stress is presented as a function of the number of impact loads applied. Since the maximum stress for impact fatigue loading is referred to the static tensile strength ($\sigma_{max}/f_0$), the relative value for one impact load is larger than unity, this being, after all, the effect of the loading rate upon the strength in the case of once-only impact loading. After 40 impact load applications this loading rate effect has been nullified, for then the relative strength has been reduced to unity. After about 5000 load applications the mean impact tensile strength has been reduced to half the static tensile strength.

The results show considerable scatter, as is indeed normally found in fatigue testing. Fig. 11, for example, shows that with once-only loading the impact tensile strength in 5% of the cases is not necessarily higher than the static tensile strength. With repeated loading the impact tensile strength in 5% of the cases has already decreased to half the static tensile strength after about 100 load applications. On the other hand, in 5% of the cases the impact tensile strength is still as high as the static tensile strength even after 1000 load applications.

In view of the range of scatter it would appear meaningful to seek an interpretation of the results for the respective mixes separately. For then the effect of the concrete composition and the direction of loading in relation to the direction of casting can be studied.

The effect of a particular parameter can be ascertained with the aid of Tables A5 and A6 of Appendix A. For this purpose the coefficients $A_1$ and $B_1$ of formula (3) or $A_2$ and $B_2$ of formula (4) are governing quantities. The test program was so planned that there were pairs of series in which only one parameter was changed, thus enabling the results to be directly compared.

The *water-cement ratio* was varied between 0.40 and 0.50 for a cement content of 375 kg per $m^3$ of concrete. From the results it emerges that for the higher water-cement ratio the relative impact tensile strength under once-only loading and also under repeated loading increases. Although the decrease in strength with the number of impact load applications is the same, the ratio between the maximum stresses after 1000 load applications and after one load application (see Table A5 of Appendix A) is 0.55 for a water-cement ratio of 0.40 (mix 23), whereas the corresponding value is 0.62 for a water-cement ratio of 0.50 (mix 25). This difference becomes even more clearly manifest if the relative strengths (see Table A6 of Appendix A) are compared: 0.63 as against 0.92. It can be inferred that the increase in tensile strength as determined by the static test and brought about by a low water-cement ratio is absent in the case of repeated impact loading.

The *cement content* was 325 kg/$m^3$ in mix 21 and 375 kg/$m^3$ in mix 25, the water-cement ratio being 0.50. The results show that the concrete with the higher cement content has a higher impact tensile strength and also undergoes less tensile strength reduction with the number of load applications. Thus the ratio between $\sigma_{max\,1000}$ and $\sigma_{max\,1}$ is 0.40 for 325 kg/$m^3$ and is 0.62 for 375 kg/$m^3$ cement content. Referred to the static value these ratios correspond to 0.56 and 0.92 respectively. What emerges therefore is that a leaner concrete is more sensitive to repeated impact loading than a con-

crete containing more cement, although both have very nearly the same cube strength (see Table A3 of Appendix A).

The *moisture content* of the concrete was varied through the storage conditions of the specimens. The "wet" specimens were immersed in water up to the time of testing, while the "dry" ones were allowed to dry for two weeks. These respective treatments were found to have virtually no effect on the tensile strength obtained with once-only impact loading.

On the other hand, the effect of the *direction of loading* in relation to the direction of casting was very pronounced. Perpendicularly to the casting direction of the concrete the impact tensile strength is higher than parallel to that direction, and in that case the decrease in impact tensile strength with increasing number of load applications is greater. The ratio between $\sigma_{\max 1000}$ and $\sigma_{\max 1}$ is the same in both cases. It can be inferred that when specimens are tested perpendicularly to the casting direction the strength is always higher than when they are tested parallel to that direction.

This description of the results will now be followed by a look at the *underlying factors* governing the behaviour observed. Fatigue is the formation of cracks which are at first stable and then grow in an unstable manner until failure occurs. For the comparison of various types of concrete the range of stable crack growth is more particularly of interest. If it is presupposed that a brittle material can undergo only very little plastic deformation, this implies that a crack – which may be a microcrack that has developed from a pore or from the contact zone between an aggregate particle and the hardened cement paste – will grow more rapidly than in a material which can deform plastically. In proportion as the concrete is more brittle, its sensitivity to repeated loading will be greater.

From the results reported above it emerges that concrete with a low water-cement ratio and a low cement content is most sensitive to decline in strength when subjected to repeated loading (impact fatigue loading). This is also the combination of influences that produce the most brittle behaviour. Having regard to the moisture content it might be supposed that wet concrete will behave in a less brittle manner and therefore attain a higher fatigue strength. Actually, this influence was evidently so slight as not to be measurable.

It can be concluded that if concrete is required to have a high impact tensile fatigue strength, it should be as tough as possible. This may mean that it is preferable to specify a lower cube (compressive) strength for the sake of obtaining greater toughness and thus higher fatigue strength.

## 4.3 *Bond tests*

### 4.3.1 General

As has been described in 3.1, the bond between the steel and the concrete was determined by tests in which a 10 mm diameter bar (or a 9.5 mm seven-wire strand) was pulled out of a concrete cylinder, the bond length being 30 mm. By keeping the bond

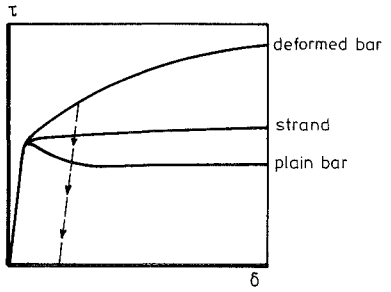


Fig. 12. $\tau$-$\delta$ relation for three steels (schematic).

length as short as possible a stress distribution that is as nearly constant as possible is obtained along the bar and is not disturbed by a high peak stress at the pull-out end of the bar and a marked drop in stress at the other end. Admittedly, this is not the stress distribution that will occur in actual practice; it must instead be regarded as an ideal situation, the results of which are suitable for the calculation of the bond stresses in practical cases. For that purpose it is necessary to know the relation between the pull-out force and the displacement between the steel and concrete.

Distinctly different force-displacement relations occur with, respectively, plain bars, deformed (ribbed) bars and strand tendons (local $\tau$-$\delta$ relations); these are shown in Fig. 12.

The three well-known bond mechanisms - namely: adhesion, friction and shear - are all present, though in varying degrees. With plain bars the adhesion is first manifest and subsequently, when this has been overcome, friction. In contrast with this, the bond between ribbed bars and concrete is due mainly to the shear resistance of the concrete between the ribs, breakdown of the bond being associated with shearing of this concrete and also with internal cracking of the concrete around the bars. The bond developed by a strand is due mainly to friction and partly to shear resistance.

The essential question with which this research was concerned was whether the local $\tau$-$\delta$ relation could be affected by the rate of loading and whether this effect, if any, would be the same for every type of steel and grade of concrete. Should there indeed be found to exist an influence exercised by the loading rate, this could be of importance with regard to the bond length of a bar embedded in concrete, the crack spacing and the crack width in a reinforced concrete structure.

The results of the tests will now first be discussed; next a formula expressing the effect of the loading rate will be established; and finally the background to the behaviour revealed by the tests will be examined.

### 4.3.2 Force-displacement relations

A pull-out test yields two primary diagrams: a force-time (or stress-time) relation and a displacement-time (or slip-time) relation.

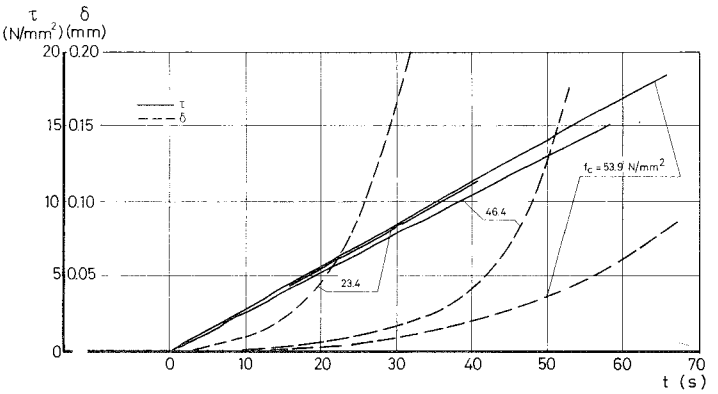


Fig. 13. Stress-time and displacement-time relations of ribbed steel at low rate, for three concretes.

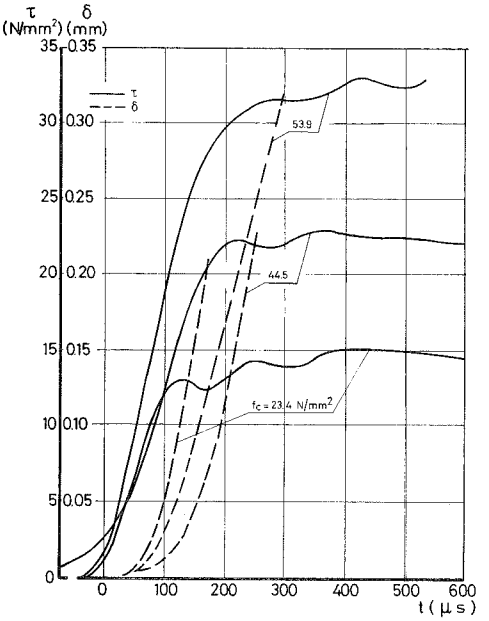


Fig. 14. Stress-time and displacement-time relations of ribbed steel at very high rate, for three concretes.

The desired force-displacement relation is obtained by synchronization of these two primary relations. Two examples of primary diagrams are given in Figs. 13 and 14: the first for a low, the second for a very high rate, in each case for three grades of concrete.

The results presented in Fig. 13 were obtained on a servo-hydraulic testing machine with force control. The bond stress-time relation is therefore a straight line, and the pull-out depends on the resistance of the bond zone. A different situation exists with regard to the results presented in Fig. 14, which were obtained with the test equipment described in 3.1. In this case, after an adjustment period has been passed, the stress-time and the displacement-time lines in a particular range are approximately straight.

Whereas the displacement-time relation continues to rise uniformly, the stress-time relations deviate at some particular time and remain almost constant. The testing method can be regarded as approximately strain-controlled.In order to arrive at comparable results, the rateof stress is defined as the slopeofthe $\tau$-$t$ line for a displacement of 0.01 mm.

These primary diagrams have been converted into $\tau$-$\delta$ relations. All the results obtained are presented in Table A7 of Appendix A. They will now be further discussed with reference to diagrams.

*Ribbed steel*

To reveal the effect of the most important variable - the loading rate - the averages of three bond stress-displacement lines at four loading rates, for a low-strength concrete, have been plotted in Fig. 15. The effect of this variable - as a parameter in the form of the relative loading rate referred to the static test - manifests itself in an increase in pull-

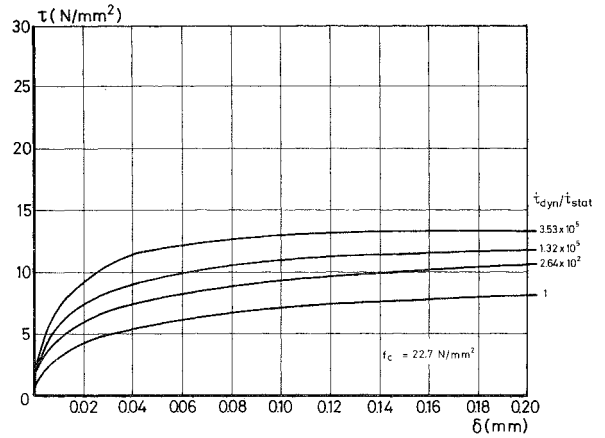


Fig. 15. $\tau$-$\delta$ relation at four loading rates for concrete with a cube strength of 22.7 N/mm$^2$.

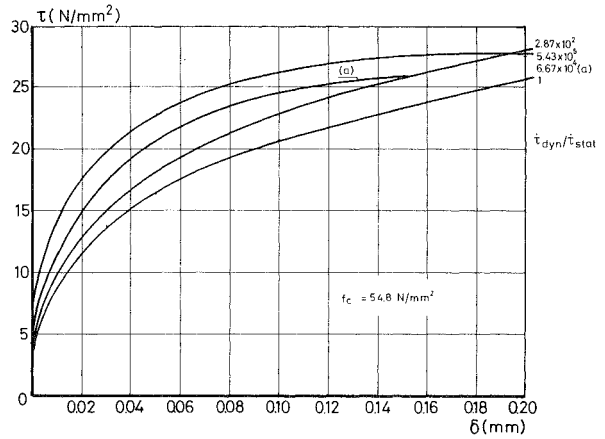


Fig. 16. $\tau$-$\delta$ relation at four loading rates for concrete with a cube strength of 54.8 N/mm$^2$.

out resistance, although the characteristic shape of the lines is preserved.

A similar effect emerges from Fig. 16, relating to a high-strength concrete. Here, too, the stiffness is greater according as the loading rate is higher, but in the absolute sense the effect of this rate is less pronounced. Because of the high cube strength the bond stresses are of course higher than for concrete of lower cube strength.

The effect of the compressive strength of the concrete is additionally illustrated in Figs. 17 and 18. The higher the compressive strength, the better the bond. This is a well-known phenomenon. But what also emerges is that the quality of the concrete (its strength class) has less effect on the bond strength according as the loading rate increases.

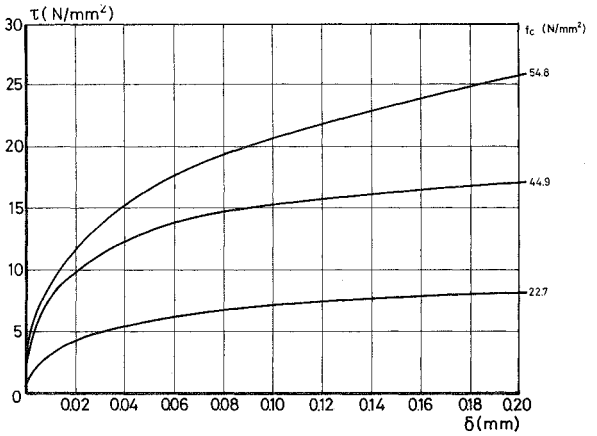


Fig. 17. $\tau$-$\delta$ relation for $\dot{\tau} = 0.3 \cdot 10^{-3}$ N/mm$^2$ · ms for three grades of concrete and ribbed steel.

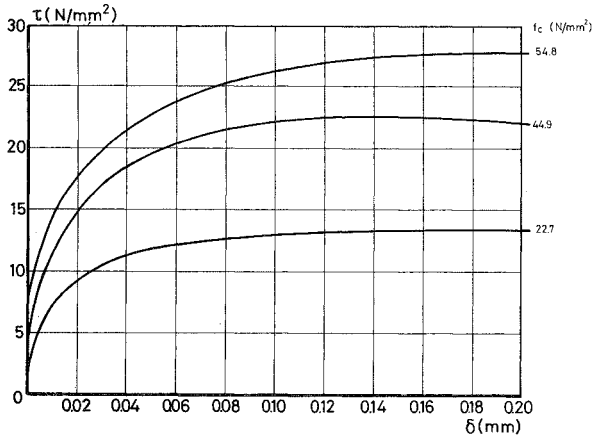


Fig. 18. $\tau$-$\delta$ relation for $\dot{\tau} \approx 140$ N/mm$^2$ · ms for three grades of concrete and ribbed steel.

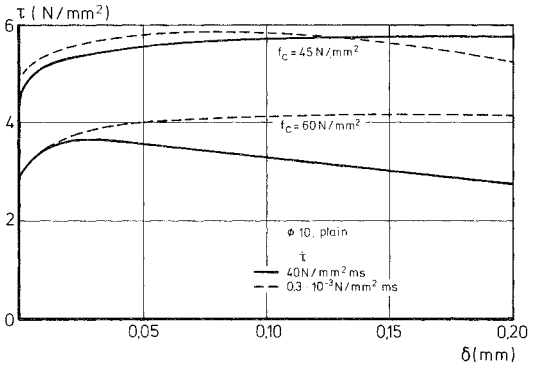


Fig. 19. $\tau$-$\delta$ relation for plain steel at two rates and for two grades of concrete.

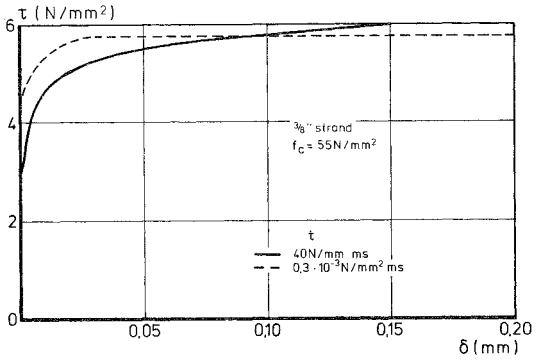


Fig. 20. $\tau$-$\delta$ relation for prestressing strand tendons at two loading rates.

*Plain steel*

Average values of $\tau$-$\delta$ relations (see Fig. 19) indicate that the loading rate has no significant effect on bond strength and bond stiffness. From the results of this research, which were in agreement with data published in the literature, it emerged that no further experimental investigations on plain steel reinforcing bars were necessary. It was concluded that such reinforcement is not sensitive to the rate of loading.

*Strand tendons*

The overall character of the results obtained with strand prestressing tendons is similar to that obtained with plain bars, i.e., the effect of the loading rate is negligible (see Fig. 20). For this reason no further investigations on strand were carried out.

### 4.3.3 Processing the results for ribbed steel

The results obtained for ribbed reinforcing bars will be processed in the same way as is done with the results of tensile tests on plain (unreinforced) concrete. A formula of the general type:

$$\frac{\tau}{\tau_0} = \left(\frac{\dot{\imath}}{\dot{\imath}_0}\right)^{\eta} \tag{5}$$

is analogous to formula (1) or (2). Here $\tau$ is the bond stress associated with a certain displacement and with a certain loading rate $\dot{\imath}$; $\tau_0$ and $\dot{\imath}_0$ are the corresponding values for the static test, while $\eta$ is the parameter which represents the effect of the compressive strength of the concrete and is a function of the displacement.

Statistical analysis of all the test results for ribbed steel yielded the following formula for

$$\eta = \frac{0{,}7(1 - 2{,}5\delta)}{f_c'^{\,0{,}8}} \tag{6}$$

where $\delta$ must be substituted in mm and $f_c'$ in N/mm$^2$. The correlation coefficient for this relation was 0.96 for the limits $0 < \delta < 0.2$ mm.

The relation between the formulae (5) and (6) expresses the fact that the bond stress for a certain displacement and a certain concrete compressive stress increases with the rate of loading. This increase is less for small displacements and low compressive strength. The bond strength is significantly dependent on the compressive strength. The effect of the loading rate upon the bond strength diminishes according as the compressive strength of the concrete is higher. As it is known that concrete is more brittle with higher compressive strength, it can alternatively be stated that the effect of the loading rate becomes less according as the concrete is more brittle in its behaviour.

In Fig. 21 the formulae (5) and (6) have been plotted in graph form for three displacements and five grades of concrete (mean cube strengths). It clearly emerges that the effect of the loading rate increases according as the concrete is of lower strength and also in cases where the displacement of the steel in relation to the concrete is small. For practical purposes this means that the effect of the loading rate is greatest immediately after the formation of a crack, for then the displacement is still small. When the crack is pulled wider open, it matters much less whether the load is applied at a faster or slower rate. Lower strength makes the concrete more sensitive to these phenomena, as is indeed expressed by formula (5).

The results of the bond tests can be explained quite simply by considering the *mechanism* of the bond between ribbed reinforcing bars and concrete. After an initial very small displacement the adhesion is destroyed and then the ribs on the bar begin to bear against the concrete. In consequence, high concentrated stresses develop under the ribs, and these stresses may exceed the cube (compressive) strength of the concrete. This in turn causes cracking within the concrete, and the ribs undergo displacement in relation to the concrete.

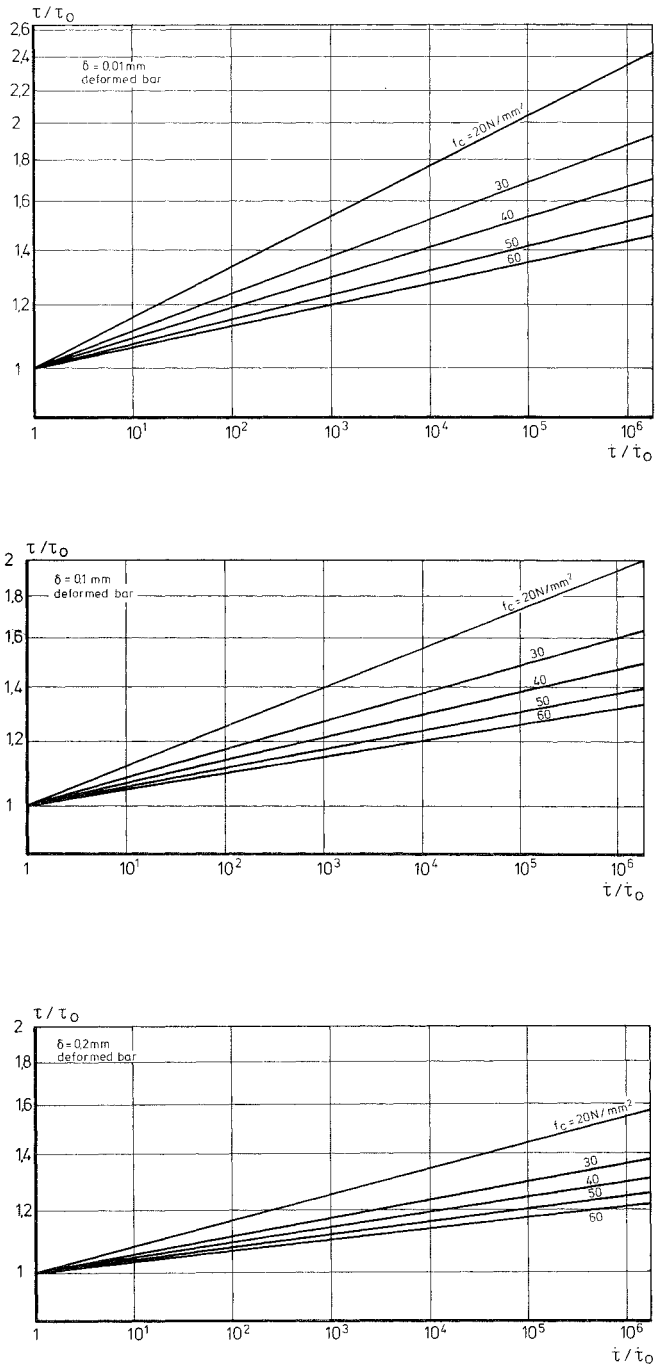


Fig. 21. Relation between bond stress, loading rate, concrete quality and displacements for ribbed steel (double logarithmic scale).

Both from the present research and from the literature it emerges that the compressive strength of the concrete and its tensile strength (cracking) are affected by the loading rate. So it is not surprising that the bond exhibits the same behaviour.

It is not possible to state with certainty to what extent this result is valid for all types of deformed reinforcement. Two aspects are, however, important in connection with assessing this: first, the fact that the value $f_R$ (relative rib surface area)* is within narrow limits for all deformed bars [15]; second, that the mechanism underlying shear bond behaviour is discernibly manifest.

The value $f_R$ is the principal parameter for bond [14] which determines, among other matters, what mechanism will govern the bond behaviour. For ribbed steel, for which $f_R$ is between 0.065 and 0.1, the mechanism as described above will develop. Hence it can be inferred that the research results are valid also for other types of deformed bars than those used in the tests, but having the above value for $f_R$. The second aspect relates to the effect of the loading rate upon the mechanical properties of concrete. As has been shown, these are sensitive to variations in the loading rate. With different reinforcing bars the loading rate will have a similar effect on bond, provided that the mechanism is the same in all cases. In view of what has been said above, it would appear justified to conclude that the research results for bond behaviour can permissibly be applied more widely than the experiments strictly authorize.

### 4.3.4 Translating the results into the behaviour for long bond lengths

With the aid of pull-out tests on specimens with short bond Rehm derived a differential equation with which the distribution of the steel stresses and bond stresses along an embedded bar can be calculated [14]. This equation, based on the linear elastic theory, is as follows:

$$\frac{d^2\delta}{dx^2} = \frac{4}{\varnothing_k} \cdot \frac{1+n\rho}{E_s} \tau(\delta) \tag{7}$$

where:

$\delta$ = displacement of steel in relation to concrete
$x$ = distance from free end of bar to section considered
$\varnothing_k$ = characteristic diameter of bar
$n$ = ratio of the moduli of elasticity of steel and concrete (modular ratio)
$\varrho$ = percentage of reinforcement
$E_s$ = modulus of elasticity of steel
$\tau(\delta)$ = bond stress as a function of displacement

---

* $f_R = \frac{A_r}{A_m}$
where $A_r$ is the projected area of the rib in the longitudinal direction of the bar and $A_m$ is the product of the bar circumference and the rib spacing.

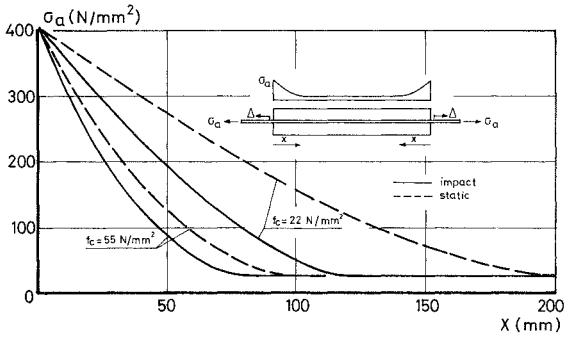


Fig. 22. Steel stresses along an embedded bar under static loading and under impact loading.

If the function $\tau(\delta)$ is also dependent on the loading rate, i.e., $\tau(\delta, \dot{\iota})$, the differential equation (7) will likewise be dependent on the loading rate.

The result of such a calculation for two types of concrete, for a given steel stress of 400 N/mm$^2$ at the free end of the bar, is shown in Fig. 22. The continuous line, which relates to impact loading, is steeper for both concretes than the dash line for static loading. This means that in the case of impact loading the steel stress decreases more rapidly on account of the higher bond stiffness and that the bond length is therefore shorter. It also means that for a high rate of loading the crack spacing in a tension member would have to be smaller and the crack width would have to be less than in the case of static load of the same magnitude. This interpretation does not take inertia effects into consideration.

## 5 Comparison with codes and standards

### 5.1 *Calculation of tensile strength from cube (compressive) strength*

If no additional tensile tests are performed on concrete, the tensile strength can be calculated from the cube strength. For this purpose there exist simple formulae derived from a large number of test results. The Netherlands code of practice for concrete VB 1974 [17] employs the following relation:

$$f_{tk} = 0.87(1 + \tfrac{1}{20} f_{ck}) \tag{8}$$

where:

$f_{tk}$ = characteristic tensile strength of the concrete
$f_{ck}$ = characteristic cube strength

The coefficient 0.87 has been introduced in order to take account of the greater scatter in the tensile strength as compared with that in the compressive strength.

The CEB-FIP Model Code [18] adopts a different relation for the purpose, namely:

$$f_{tm} = 0.26 f_{ck}^{2/3} \tag{9}$$

where:

$f_{tm}$ = mean tensile strength of the concrete
$f_{ck}$ = characteristic cube strength

In a general way the formulae (8) and (9) can be written respectively as follows:

$$f_{tk} = a + bf_{ck} \tag{10}$$

$$f_{tm} = cf_{ck}{}^{d} \tag{11}$$

The coefficients $a$, $b$, $c$ and $d$ comprise all the factors that may affect the ratio between tensile and compressive strength, e.g., the composition of the concrete, the temperature, the moisture content of the test specimen, the method of testing and the rate of loading.

If the true effect of the loading rate were introduced, then either the above-mentioned coefficients could be made rate-dependent or an extra term be added to take account of the loading rate. The former alternative appears attractive because the known relation between cube strength and tensile strength of concrete then remains unchanged, only the numerical values being somewhat changed. In that case, however, it is presupposed that there exists a close relation between tensile strength and compressive strength at high loading rates. In the course of the research this was found not to be entirely so; other parameters, such as the water-cement ratio and the cement content, resulted in better correlation than the cube strength did.

Retaining the simple relation between tensile strength and compressive strength for practical convenience implies that the scatter of the ratios must increase with increasing rate of loading. This phenomenon can be allowed for by so determining the coefficients that the lower results are given more weight than the higher ones. This is a safe approximation that underrates some results.

There is another aspect that must be given attention in connection with the determination of the coefficients in the formulae (10) and (11). In the research, particular concrete mix compositions were employed, which resulted in particular mean values and standard deviations. Because of the limited scope of the investigations and the fact that the scatter of laboratory tests differs from that of tests conducted under practical conditions, it is not possible to calculate the characteristic values. The coefficients are accordingly determined with the aid of the mean values.

Taking account of the two above-mentioned aspects, the following formulae were established, for which purpose it was attempted to round off the coefficients to values that could be conveniently memorized. Thus the VB formula becomes:

static, $\dot{\sigma}_0$ $\qquad f_{bm} = 0.87(1 + \frac{1}{20} f_{cm})$ (12a)

$\frac{\dot{\sigma}}{\dot{\sigma}_0} = 10^3$ $\qquad f_{bm} = 0.87(3.15 + \frac{1}{40} f_{cm})$ (12b)

$\frac{\dot{\sigma}}{\dot{\sigma}_0} = 10^6$ $\qquad f_{bm} = 0.87(4.60 + \frac{1}{80} f_{cm})$ (12c)

$f_{bm}$ and $f_{cm}$ are the mean values of the static tensile strength and of the static compressive strength (cube strength) of concrete respectively (in N/mm$^2$).

The CEB-FIP formula is modified to the following:

$$\text{static, } \dot{\sigma}_0 \qquad f_{bm} = 0.26(f_{cm} - 10)^{2/3} \tag{13a}$$

$$\frac{\dot{\sigma}}{\dot{\sigma}_0} = 10^3 \qquad f_{bm} = 1.00(f_{cm} - 10)^{2/5} \tag{13b}$$

$$\frac{\dot{\sigma}}{\dot{\sigma}_0} = 10^6 \qquad f_{bm} = 2.40(f_{cm} - 10)^{1/5} \tag{13c}$$

According to the CEP-FIP Model Code the factor $(f_{cm} - 10)$ is equal to the characteristic value. It is possible to interpolate for other loading rates than those indicated.

The formulae (12) and (13) are presented graphically in Fig. 23. Both express the facts that emerged from the investigations, namely, that the tensile strength increases with higher loading rate, but also that this increase becomes less pronounced with higher strength of the concrete (greater brittleness). For a loading rate which is $10^6$ times as high as in the static test (i.e., 100 N/mm$^2$ · ms) the impact tensile strength is doubled for a mean cube strength of 30 N/mm$^2$ and is increased 1.5-fold for a mean cube strength of 50 N/mm$^2$. Fig. 23 also shows that the CEB-FIP formula always predicts higher values than the VB formula.

A comparison between the proposed conversion value and the results obtained from the regression analysis with the aid of which the test results were processed is made possible in Fig. 24. It emerges that the VB line gives a good approximation of the static results and that the tensile strength at higher loading rates is underestimated. This latter aspect is intentional, however, in view of the not very close relation between compressive strength and tensile strength. The CEB-FIP line overestimates the static strength, at least in this calculation with the constant difference of 10 N/mm$^2$ between the mean and the characteristic value for the compressive strength. For $\dot{\sigma} = 10^{-1}$ N/mm$^2$ · ms the

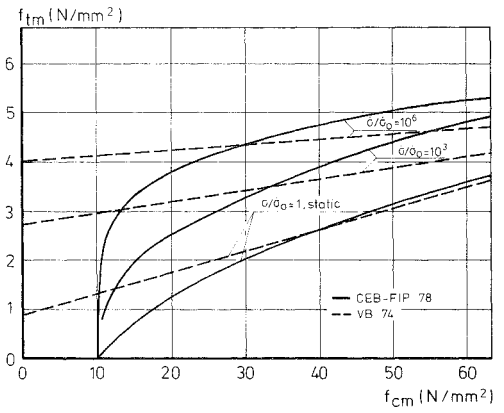


Fig. 23. Relation between concrete tensile strength and cube strength according to VB formulae (12) en CEB-FIP formulae (13) at three loading rates.

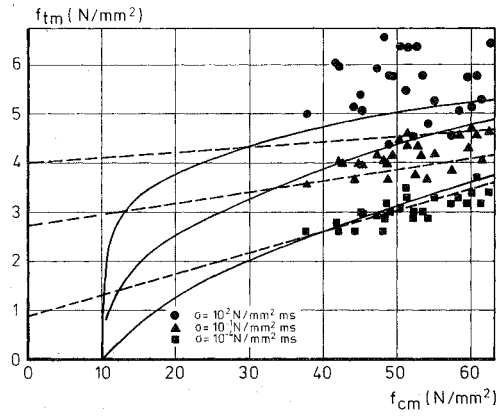


Fig. 24. Comparison of experimental results with the relation between concrete tensile strength and cube strength according to VB formulae (12) and CEB-FIP formulae (13) at three loading rates.

CEB-FIP line likewise overestimates the results. Only for $\dot{\sigma} = 10^2$ N/mm$^2$ · ms does the relation appear to be closer to reality, but in view of what has been noted above this, too, is to be regarded as something of an overestimation.

A better representation of the test results is obtained with the CEB-FIP formula if the difference between the mean and the characteristic compressive strength is incorporated in the coefficient $c$ and not taken into account merely by applying a shift of 10 N/mm$^2$ to the compressive strength axis. From Table 2.2 in the CEB-FIP Model Code's explanatory notes it can be deduced that:

$$f_{t\,0.05} \approx 0.75 f_{tm} \tag{14}$$

Let $f_{t\,0.05}$ be designated as the characteristic strength; then:

$$f_{tk} \approx 0.75 \cdot 0.26 f_{ck}^{2/3} \tag{15}$$

or:

$$f_{tk} \approx 0.20 f_{ck}^{2/3} \tag{16}$$

Associated with formula (16) are two statistically similar values. If this same expression is used also for mean values - as in the VB formula - then the formulae (13) are converted into the following relations:

$$\text{static, } \dot{\sigma}_0 \qquad f_{tm} = 0.20 f_{cm}^{2/3} \tag{17a}$$

$$\frac{\dot{\sigma}}{\dot{\sigma}_0} = 10^3 \qquad f_{tm} = 1.10 f_{cm}^{1/3} \tag{17b}$$

$$\frac{\dot{\sigma}}{\dot{\sigma}_0} = 10^6 \qquad f_{tm} = 3.10 f_{cm}^{1/10} \tag{17c}$$

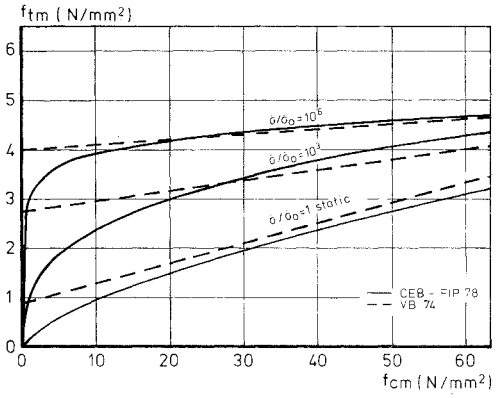


Fig. 25. Relation between concrete tensile strength and cube strength according to VB formulae (12) and modified CEB-FIP formulae (17) at three loading rates.

From Fig. 25 it emerges that this modified CEB-FIP line yields almost the same results as the VB line does and thus provides a better representation of the test results, i.e., adopts a more conservative approach.

It is proposed that either the formulae (12) based on the VB 1974 Netherlands code for concrete or the formulae (17) based on the CEB-FIP Model Code be adopted, in which case the same functions can be used for calculating the mean values or the characteristic values, depending in whether the mean or the characteristic value is introduced for the cube (compressive) strength.

### 5.2 *Repeated impact tensile loading*

The tensile strength under repeated impact loading is especially of importance for structures which have to be uncracked under service conditions. An example of such a structure is a concrete road. Fig. 26 shows a Smith diagram which is used in concrete road pavement design and in which the upper stress limit and the mean stress are presented in relation to the short-term strength. The continuous lines relate to short-term tests, while the dash lines indicate the effect of long-term (sustained) loading.

The factor 0.8 is the ratio between sustained load strength and short-term strength. For a zero lower stress limit, according to these diagrams, a fatigue strength of $0.5f_0$ can be expected (for $N = 2 \times 10^6$ cycles). For $N = 100$ this would be $0.8f_0$. All these values are based on test results obtained at normal rates of loading.

The mean values of the results obtained with repeated impact tensile loading are included in Fig. 26. It emerges, first, that for a low number of load applications the results are higher than in the case of normal loading rate; second, that the effect of the number of load applications is much greater for impact loading. For $10^3$ load applications the results are already lower, and for $10^4$ load applications the strength attains only $0.42f_0$.

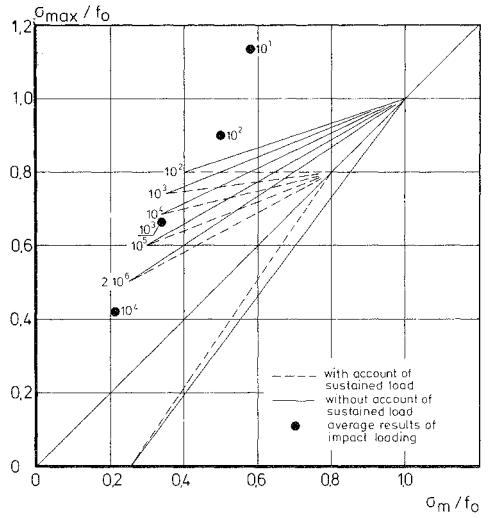


Fig. 26. Smith diagram for repeated tensile loading of concrete.

In general it can be inferred from these results that the diagrams which can be used for normal loading rates give too favourable a picture of the behaviour under repeated impact loading. At high loading rates concrete is evidently more sensitive to repeated loading.

### 5.3 *Bond*

In the VB 1974 and in the CEB-FIP Model Code the bond strength is given as a linear function of the tensile strength, bond strength being defined for the present purpose as the average bond stress along the anchorage length of a bar loaded to a stress equal to the yield point of the steel. This cannot be directly compared with the values which, in the present research, were obtained for short bond lengths. For this reason, too, it is not possible to give a similar quantitative relation.

It can, however, be proposed to use the formulae for static values, for which purpose the static tensile strength is replaced by the tensile strength associated with a particular loading rate. This last-mentioned strength can be obtained either from Fig. 25 or from the formulae (12) and (17).

From a comparison of Figs. 25 and 21 it can be inferred that this procedure will lead to acceptable results. In both diagrams the increase in tensile strength with higher-strength concrete and higher loading rate shows the same trend. The order of magnitude of the increase is also in agreement. Only the fact that the ratio $\tau/\tau_0$ is dependent on the absolute displacement (small displacement, large effect) rules out an exact quantitative comparison.

This proposal is valid only for deformed (ribbed) reinforcing bars. In the investiga-

tions for plain bars and for strand prestressing tendons no effect of the loading rate was found, and it is accordingly recommended that for these types of steel the static values should always be adopted in the calculations, irrespective of the rate of loading.

## 6 Summary and conclusions

In connection with the increasing need for information on the effect of the loading rate upon the mechanical properties of concrete, experimental research on the axial tensile strength of concrete and on the bond between reinforcement and concrete was carried out.

In order to attain very high loading rates - up to 600 000 times as high as those normally applied in „static" loading tests - a special testing rig, based on the Split Hopkinson Bar principle, was developed and built. The same rig can, after some simple adaptation, also be used for pull-out tests for measuring the bond between steel and concrete within 200 μs.

The investigation comprised three parts:

- determination of the uniaxial tensile strength and the stress-strain diagram of concrete under single impact tensile loading;
- determination of the uniaxial tensile strength of concrete under repeated impact tensile loading;
- determination of the bond behaviour between steel and concrete under single impact tensile loading.

In the first part of this research program the following parameters were investigated:

- loading rate;
- type of cement;
- cement content;
- water-cement ratio;
- maximum size of aggregate particles;
- moisture condition of concrete;
- loading/casting direction.

From all the test results it emerges that the rate of loading has a significant effect on the tensile strength of concrete. The tensile strength increases with the loading rate and the relationship between them is double-logarithmic. For example, when concrete is loaded a million times as faster than in the static test, the mean tensile strength can be expected to be 80% higher. Actually this value ranges between 35 and 110% and depends on the introduced test parameters as follows:

- type of cement: no distinct effect;
- water-cement ratio: a higher water-cement ratio results in higher values of the ratio impact/static tensile strength;
- cement content: a combination of a higher cement content and a higher water-cement ratio seems to result in a higher relative impact tensile strength;

- maximum size of aggregate particles: larger particles result in a lower relative impact tensile strength;
- moisture condition of concrete: no distinct effect;
- loading/casting direction: loading perpendicularly to the casting direction results in higher values of the relative impact tensile strength.

The stress-strain diagram of concrete under impact tensile loading shows an initially steeper slope and a larger ultimate strain than the diagram obtained under static loading. This means that the behaviour of concrete does not become more brittle with increasing rate of loading.

Repeated impact tensile loading appeared to have a great influence on impact tensile strength. After 100 loading cycles the gain in strength due to the high loading rate vanishes, and after ca. 1 000 impacts the tensile strength is reduced to only 70% of the static strength. These mean values, too, are dependent on the composition of the concrete. Thus, a higher water-cement ratio and a high cement content are favourable to the impact tensile strength under repeated loading, while the moisture content of the concrete has no effect. Load application at right angles to the direction of concreting results in higher fatigue strength. In this part of the research the loading rate was kept constant.

In investigating the background to these phenomena it is necessary to consider the process of crack growth in the concrete. According as the hardened cement paste is more brittle, failure will occur more easily under repetitive loading, and according as the loading rate increases, influences such as crack branching and forced fracturing of particles will become more important.

The bond resistance between reinforcement and concrete was investigated by means of pull-out tests with short embedment length. The variables in this investigation were the type of steel, the cube compressive strength of concrete and the rate of pull-out. It was found that the influence of loading rate on the bond resistance of deformed bars was similar to that on the tensile strength of concrete. For plain bars and prestressing strands this effect is negligible. The loading rate has the greatest effect in the case of low strength concretes, especially at small displacements between reinforcing steel and concrete. This result can be interpreted such that the effective bond length of a deformed bar decreases with increasing loading rate.

After the analysis of experimental results it was attempted to extend the relation between tensile strength and cube compressive strength of concrete – as conceived in the Netherlands code VB 1974 and in the CEB-FIP Recommendations – to comprise the rate of loading. Having due regard to the scatter displayed by the results, a proposal for a linear relationship and for a non-linear relationship is made, for which the coefficients are introduced as dependent on the rate of loading.

The results of repeated impact loading tests were compared with those of normal fatigue tests. It emerged that the commonly employed Smith diagrams would give too favourable picture for impact fatigue.

Considering bond resistance it is proposed that the relationships given in VB 1974

and in the CEB-FIP Recommendations should be used. The effect of the rate of loading can be neglected for plain bars and for prestressing strands. For deformed bars subjected to monotonically increasing load, however, the tensile strength associated with a particular loading rate should be used instead of the static tensile strength.

For applying the results of this research in actual practice the relevant cases would include the shear strength of slabs and beams under impact loading, the punching shear strength of slabs, the crack width, the crack spacing and the deflection of reinforced concrete structural members. By means of large-scale investigations [21] it has been shown that impact loads cause an increase in the magnitude of the failure load, in accordance with the results of this research. Another relevant possibility is to reinforce foundation piles in order to prevent brittle fracture.

Taking account of the complexity of this problem it does not appear appropriate to introduce the impact tensile strength values into the commonly used formulae before investigations will show how that should be done. This fact leads to a suggestion for further research: to investigate the behaviour of piles during pile-driving, both theoretically and experimentally, with particular reference to the behaviour during and after cracking. Another direction in which research may be continued is that of the multi-dimensional behaviour of concrete under impact loading. This in order to establish a failure criterion for concrete at high rates of loading. When that problem will be solved for ordinary concrete, attention must be turned to fibre-reinforced concrete and polymer concrete, since these concretes may have a significant part to play in structures which can be subjected to impact and explosion loads.

## 7 Notations

| | |
|---|---|
| $a, b, c, d$ | coefficients |
| $f$ | tensile strength |
| $f_0$ | static tensile strength |
| $f_{tk}$ | calculated characteristic tensile strength of concrete |
| $f_{tm}$ | calculated mean tensile strength of concrete |
| $f_c$ | cube strength (compressive strength) |
| $f_{cm}$ | mean cube strength |
| $f_{ck}$ | characteristic cube strength |
| $\tau(\delta)$ | bond stress as function of displacement |
| $n$ | number of test specimens |
| $n$ | modular ratio of steel and concrete |
| $r$ | correlation coefficient |
| $x$ | coordinate |
| $A, B$ | coefficients |
| $E$ | modulus of elasticity |
| $N$ | number of load applications to failure |
| $\beta$ | coefficient |
| $\delta$ | displacement (pull-out) |
| $\varepsilon$ | strain |
| $\dot{\varepsilon}$ | strain rate |
| $\eta$ | coefficient |
| $\varrho$ | reinforcement percentage |
| $\sigma$ | stress |
| $\dot{\sigma}$ | loading rate (stress rate) |
| $\dot{\sigma}_0$ | loading rate in static test |
| $\sigma_{\max}$ | upper stress limit for repeated loading |
| $\tau$ | bond stress for a certain displacement |
| $\tau_0$ | bond stress in static test |
| $\dot{\tau}$ | loading rate for bond |
| $\dot{\tau}_0$ | loading rate in static bond test |
| $\varnothing_k$ | characteristic diameter of a plain or a deformed bar |

## 8 References


1. KOMLOŠ, K., Investigation of rheological properties of concrete in uniaxial tension. Materialprüfung 1970, nr. 9, pp. 300-304.
2. HEILMANN, H. G., H. HILFSDORF and K. FINSTERWALDER, Festigkeit und Verformung von Beton unter Zugspannungen. Deutscher Ausschuss für Stahlbeton, Heft 203, Berlin 1977.
3. TAKEDA, J. and H. TACHIKAWA, Deformation and fracture of concrete subjected to dynamic load. Proceedings International Conference „Mechanical behaviour of materials", Kyoto 1971, Vol. IV.
4. KVIRIKADZE, O. P., Determination of the ultimate strength and modulus of deformation of concrete at different rates of loading. International Symposium „Testing in situ of concrete structures", Budapest 1977, pp. 109-117.
5. BIRKIMER, D. L. and R. LINDEMANN, Dynamic tensile strength of concrete materials. Journal of the American Concrete Institute, title no. 68-8, January 1971.
6. HJORTH, O., Ein Beitrag zur Frage der Festigkeiten und des Verbundverhaltens von Stahl und Beton bei hohen Beanspruchungsgeschwindigkeiten. Dissertation Technische Universität Braunschweig, 1976.
7. HANSEN, R. J. and A. A. LIEPINS, Behaviour of bond under dynamic loading. Journal of the ACI (1962), no. 4, pp. 563-583.
8. FAGERLUND, G. and B. LARSSON, Betongs slaghallfasthet. Cement- och betonginstitutet, Forskning Fo 4:79, Stockholm 1979.
9. MIHASHI, H. and M. A. IZUMI, Stochastic theory for concrete fracture. Cement and Concrete Research 7 (1977), pp. 411-422.
10. MIHASHI, M. and F. H. WITTMANN, Stochastic approach to study the influence of rate of loading on strength of a concrete. HERON 25 (1980) no. 3.
11. KOLSKY, H., An investigation of the mechanical properties of materials at very high rates of loading. Proceedings Phys. Soc. Sec. B62, (1949), pp. 676-700.
12. STROEVEN, P., Some aspects of the micromechanics of concrete. Dissertation Delft University of Technology, 1973.
13. MCCLINTOCK, F. A. and A. S. ARGON, Mechanical behaviour of materials. Addison-Wesley, Reading, U.S.A., 1966.
14. MARTIN, H. and P. NOAKOWSKI, Verbundverhalten von Betonstählen. Aus unseren Forschungsarbeiten IV, Technische Universität München, December 1978, pp. 75-77.
15. REHM, G., Über die Grundlagen des Verbundes zwischen Stahl und Beton, Deutscher Ausschuss für Stahlbeton, Heft 138, Berlin 1961.
16. EISENMANN, J., Betonfahrbahnen. Wilhelm Ernst & Sohn, Berlin/München 1979.
17. Voorschriften Beton VB 1974, NEN 3861, Nederlandse Normalisatie-instituut (Netherlands Standard Institute), Delft.
18. CEB-FIP Model Code for Concrete Structures. Comité Euro-International du Béton, Paris 1978.
19. KÖRMELING, H. A., A. J. ZIELINSKI and H. W. REINHARDT, Experiments on concrete under single and repeated uniaxial impact tensile loading. Stevin report 5-80-3, Delft University of Technology, May 1980.
20. VOS, E. and H. W. REINHARDT, Bond resistance of deformed bars, plain bars and strands under impact loading. Stevin report 5-80-6, Delft University of Technology, September 1980.
21. Symposium „Stossbeanspruchung von Betonkonstruktionen", Universität Dortmund, September 1980.

## Appendix A

Table A1. Grading of aggregates with different maximum grain size

| sieves acc. to NEN 2570 sieve size (mm) | cumulative percentage retained (m/m) at maximum grain size | | |
|---|---|---|---|
| | 8 mm | 16 mm | 24 mm |
| 24 | - | - | - |
| 16 | - | - | 31 |
| 8 | - | 29 | 60 |
| 4 | 30 | 50 | 78 |
| 2 | 50 | 64 | 80 |
| 1 | 65 | 75 | 90 |
| 0,5 | 80 | 82 | 94 |
| 0,25 | 93 | 95 | 97 |
| 0,125 | 100 | 100 | 100 |

Table A2. Composition and results of the control tests on the concrete of the preliminary program

| | | | | | cube strength | | splitting tensile strength | |
|---|---|---|---|---|---|---|---|---|
| mix | cement content (kg/m$^3$) | maximim particle size (mm) | type of cement | water-cement ratio | $f_{cm}$ (N/mm$^2$) | coefficient of variation (%) | $f_{spl}$ (N/mm$^2$) | coefficient of variation (%) |
| 1 | 325 | 16 | PA | 0,45 | 51,04 | 4,1 | 3,52 | 11,1 |
| 2 | 325 | 24 | PB | 0,45 | 52,15 | 1,6 | 2,95 | 5,4 |
| 3 | 375 | 24 | PB | 0,40 | 57,05 | 2,3 | 3,20 | 15,6 |
| 4 | 375 | 24 | PB | 0,45 | 48,28 | 3,9 | 3,24 | 9,9 |
| 5 | 325 | 16 | PB | 0,45 | 47,05 | 3,2 | 2,93 | 8,5 |
| 6 | 375 | 16 | PB | 0,40 | 53,53 | 3,4 | 2,97 | 6,4 |
| 7 | 375 | 16 | PB | 0,45 | 50,09 | 3,4 | 3,18 | 17,9 |
| 8 | 325 | 16 | PC | 0,45 | 60,84 | 1,2 | 3,66 | 7,4 |
| 9 | 375 | 16 | PC | 0,40 | 62,53 | 1,2 | 3,38 | 6,8 |
| 10 | 316 | 16 | PB1A | 0,48 | 43,82 | 3,1 | 2,65 | 6,4 |
| 11 | 316 | 16 | PB1B | 0,45 | 49,14 | 2,2 | 3,03 | 11,5 |
| 12 | 364 | 16 | PB1B | 0,41 | 52,24 | 1,9 | 3,03 | 4,3 |
| 13 | 358 | 16 | PB1B | 0,45 | 51,10 | 3,6 | 3,37 | 4,7 |
| 14 | 290 | 16 | PA | 0,52 | 37,23 | 4,2 | 2,58 | 10,1 |
| 15 | 325 | 8 | PB | 0,48 | 41,51 | 0,8 | 2,79 | 6,4 |
| 16 | 375 | 8 | PB | 0,43 | 47,96 | 3,8 | 2,63 | 5,7 |
| 17 | 352 | 8 | PB | 0,48 | 41,60 | 4,7 | 2,69 | 4,5 |
| 18 | 375 | 16 | PC | 0,45 | 59,78 | 2,8 | 3,25 | 7,4 |

Table A3. Composition and results of the control tests on the concrete of the main program

| mix | cement content ($kg/m^3$) | maximum particle size (mm) | moisture condition | water-cement ratio | cube strength $f_{cm}$ ($N/mm^2$) | cube strength coefficient of variation (%) | splitting tensile strength $f_{spl}$ ($N/mm^2$) | splitting tensile strength coefficient of variation (%) |
|---|---|---|---|---|---|---|---|---|
| 19 | 325 | 16 | dry | 0,40 | 61,14 | 1,4 | 3,33 | 9,6 |
| 20 | 325 | 16 | wet | 0,40 | 60,10 | 0,9 | 3,44 | 8,7 |
| 21* | 325 | 16 | dry | 0,50 | 47,80 | 6,2 | 2,95 | 10,0 |
| 22* | 325 | 16 | wet | 0,50 | 44,79 | 5,5 | 3,00 | 11,3 |
| 23* | 375 | 16 | dry | 0,40 | 58,25 | 6,3 | 3,31 | 10,1 |
| 24 | 375 | 16 | wet | 0,40 | 54,66 | 7,2 | 3,50 | 16,0 |
| 25* | 375 | 16 | dry | 0,50 | 45,73 | 3,4 | 3,06 | 9,7 |
| 26 | 350 | 8 | dry | 0,40 | 54,20 | 4,2 | 2,88 | 5,7 |

* used also for repeated impact loading

Table A4. Calculated values of the impact tensile strength, obtained from the regression analysis based on: $\ln f = A + B \ln \dot{\sigma}$.

| mix | number of tests | regression coefficient | | | 95% confidence belt for | | impact tensile strength for a loading rate $\dot{\sigma}$ in $N/mm^2 \cdot ms$ | | | |
|---|---|---|---|---|---|---|---|---|---|---|
| | results | $A$ | $B$ | $r^2$ | $\ln f$ | $B$ | $\dot{\sigma} = 0{,}0001$ ($N/mm^2$) | $\dot{\sigma} = 3$ ($N/mm^2$) | $\dot{\sigma} = 30$ ($N/mm^2$) | $\frac{f(\dot{\sigma}=30)}{f(\dot{\sigma}=0{,}0001)}$ |
| 1 | 9 | 1,552 | 0,0324 | 0,87 | ± 0,182 | ± 0,0106 | 3,50 | 4,89 | 5,27 | 1,50 |
| 2 | 9 | 1,375 | 0,0320 | 0,81 | ± 0,223 | ± 0,0135 | 2,94 | 4,10 | 4,41 | 1,50 |
| 3 | 10 | 1,407 | 0,0276 | 0,70 | ± 0,254 | ± 0,0145 | 3,17 | 4,21 | 4,49 | 1,42 |
| 4 | 9 | 1,367 | 0,0226 | 0,53 | ± 0,315 | ± 0,0185 | 3,19 | 4,02 | 4,24 | 1,33 |
| 5 | 9 | 1,546 | 0,0520 | 0,95 | ± 0,172 | ± 0,0101 | 2,91 | 4,97 | 5,60 | 1,92 |
| 6 | 9 | 1,538 | 0,0495 | 0,96 | ± 0,157 | ± 0,0092 | 2,95 | 4,92 | 5,51 | 1,87 |
| 7 | 9 | 1,623 | 0,0521 | 0,91 | ± 0,247 | ± 0,0146 | 3,14 | 5,37 | 6,05 | 1,93 |
| 8 | 9 | 1,604 | 0,0329 | 0,82 | ± 0,233 | ± 0,0136 | 3,67 | 5,15 | 5,56 | 1,52 |
| 9 | 9 | 1,652 | 0,0471 | 0,92 | ± 0,201 | ± 0,0118 | 3,38 | 5,49 | 6,12 | 1,81 |
| 10 | 8 | 1,418 | 0,0486 | 0,95 | ± 0,165 | ± 0,0103 | 2,64 | 4,35 | 4,87 | 1,84 |
| 11 | 9 | 1,538 | 0,0487 | 0,83 | ± 0,332 | ± 0,0194 | 2,97 | 4,91 | 5,49 | 1,85 |
| 12 | 9 | 1,606 | 0,0539 | 0,98 | ± 0,121 | ± 0,0070 | 3,03 | 5,29 | 5,98 | 1,97 |
| 13 | 9 | 1,638 | 0,0471 | 0,87 | ± 0,252 | ± 0,0158 | 3,33 | 5,42 | 6,04 | 1,81 |
| 14 | 9 | 1,392 | 0,0483 | 0,80 | ± 0,336 | ± 0,0210 | 2,58 | 4,24 | 4,74 | 1,84 |
| 15 | 9 | 1,543 | 0,0566 | 0,96 | ± 0,163 | ± 0,0102 | 2,78 | 4,98 | 5,67 | 2,04 |
| 16 | 8 | 1,576 | 0,0675 | 0,96 | ± 0,205 | ± 0,0132 | 2,60 | 5,21 | 6,08 | 2,34 |
| 17 | 9 | 1,535 | 0,0590 | 0,99 | ± 0,083 | ± 0,0052 | 2,69 | 4,95 | 5,67 | 2,11 |
| 18 | 9 | 1,563 | 0,0424 | 0,87 | ± 0,225 | ± 0,0142 | 3,23 | 5,00 | 5,51 | 1,71 |
| 19 | 11 | 1,492 | 0,0370 | 0,93 | ± 0,140 | ± 0,0073 | 3,16 | 4,63 | 5,04 | 1,59 |
| 20 | 14 | 1,504 | 0,0311 | 0,85 | ± 0,179 | ± 0,0083 | 3,38 | 4,65 | 5,00 | 1,48 |
| 21 | 15 | 1,526 | 0,0519 | 0,91 | ± 0,205 | ± 0,0100 | 2,84 | 4,87 | 5,49 | 1,93 |
| 22 | 15 | 1,493 | 0,0431 | 0,90 | ± 0,173 | ± 0,0084 | 3,00 | 4,66 | 5,15 | 1,72 |
| 23 | 26 | 1,482 | 0,0322 | 0,80 | ± 0,196 | ± 0,0068 | 3,28 | 4,56 | 4,91 | 1,50 |
| 23* | 22 | 1,599 | 0,0447 | 0,90 | ± 0,186 | ± 0,0069 | 3,27 | 5,20 | 5,77 | 1,76 |
| 24 | 19 | 1,507 | 0,0350 | 0,77 | ± 0,213 | ± 0,0098 | 3,27 | 4,69 | 5,08 | 1,55 |
| 25 | 38 | 1,457 | 0,0374 | 0,84 | ± 0,183 | ± 0,0055 | 3,05 | 4,47 | 4,87 | 1,60 |
| 26 | 7 | 1,401 | 0,0373 | 0,92 | ± 0,208 | ± 0,0130 | 2,89 | 4,23 | 4,60 | 1,59 |
| 26* | 13 | 1,533 | 0,0513 | 0,90 | ± 0,209 | ± 0,0115 | 2,89 | 4,90 | 5,51 | 1,91 |

* loading direction perpendicular to casting direction

Table A5. Calculated values of the strength after repeated loading, obtained from the regression analysis based on: $\sigma_{max} = A + B \ln N$.

| mix | number of test results | regression coefficients $A$ | $B$ | $r^2$ | 95% confidence belt for $\sigma_{max}$ | 95% confidence belt for $B$ | impact tensile strength after $N$ load applications (N/mm²) $N=1$ | $N=10$ | $N=100$ | $N=1000$ | $\frac{\sigma_{max}(N=1000)}{\sigma_{max}(N=1)}$ |
|---|---|---|---|---|---|---|---|---|---|---|---|
| 21 | 13 | 4,142 | −0,360 | 0,72 | ± 1,580 | ± 0,150 | 4,14 | 3,31 | 2,48 | 1,65 | 0,40 |
| 22 | 14 | 4,512 | −4,080 | 0,80 | ± 1,343 | ± 0,131 | 4,51 | 3,57 | 2,63 | 1,69 | 0,37 |
| 23 | 35 | 3,757 | −0,242 | 0,65 | ± 0,808 | ± 0,063 | 3,76 | 3,20 | 2,64 | 2,08 | 0,55 |
| 23* | 7 | 5,649 | −0,356 | 0,93 | ± 0,596 | ± 0,116 | 5,65 | 4,83 | 4,01 | 3,19 | 0,56 |
| 25 | 16 | 4,513 | −0,245 | 0,78 | ± 0,674 | ± 0,075 | 4,51 | 3,95 | 3,38 | 2,82 | 0,62 |

* loading direction perpendicular to casting direction

Table A6. Calculated values of the strength after repeated loading, obtained from the regression analysis based on: $\sigma_{max}/f_0 = A + B \ln N$

| mix | number of test results | regression coefficients $A$ | $B$ | $r^2$ | 95% confidence belt for $\frac{\sigma_{max}}{f_{spl}}$ | 95% confidence belt for $B$ | relative impact tensile strength after $N$ load applications (N/mm²) $N=1$ | $N=10$ | $N=100$ | $N=1000$ |
|---|---|---|---|---|---|---|---|---|---|---|
| 21 | 13 | 1,404 | −0,122 | 0,72 | ± 0,535 | ± 0,051 | 1,40 | 1,12 | 0,84 | 0,56 |
| 22 | 14 | 1,504 | −0,136 | 0,80 | ± 0,447 | ± 0,041 | 1,50 | 1,19 | 0,88 | 0,56 |
| 23 | 35 | 1,135 | −0,073 | 0,65 | ± 0,144 | ± 0,018 | 1,13 | 0,97 | 0,80 | 0,63 |
| 23* | 7 | 1,706 | −0,108 | 0,93 | ± 0,180 | ± 0,033 | 1,71 | 1,46 | 1,21 | 0,96 |
| 25 | 16 | 1,475 | −0,080 | 0,78 | ± 0,220 | ± 0,023 | 1,47 | 1,29 | 1,11 | 0,92 |

* loading direction perpendicular to casting direction

Table A7. Results of the pull-out tests

| type of steel | code* | mix | cube strength ($N/mm^2$) | splitting tensile strength ($N/mm^2$) | modulus of elasticity ($N/mm^2$) | bond stress $\tau$ for displacement $\delta =$ .. mm | | | | | | loading rate ($N/mm^2 \cdot ms$) | behaviour at failure** |
|---|---|---|---|---|---|---|---|---|---|---|---|---|---|
| | | | | | | 0,01 ($N/mm^2$) | 0,03 ($N/mm^2$) | 0,05 ($N/mm^2$) | 0,10 ($N/mm^2$) | 0,15 ($N/mm^2$) | 0,20 ($N/mm^2$) | | |
| ribbed steel, ø 10 | 0806 | 1 | 23,4 | 2,00 | 30,9 | 8,32 | 11,34 | 12,60 | 13,27 | 13,27 | 12,85 | 108 | 1 |
| | 0812 | 1 | 23,4 | 2,00 | 30,9 | 6,50 | 9,62 | 10,96 | 12,32 | 12,90 | 13,19 | 104 | 1 |
| | 0807 | 1 | 23,4 | 2,00 | 30,9 | 6,17 | 9,07 | 10,38 | 11,42 | 11,80 | 11,70 | 50,1 | 1 |
| | 0808 | 1 | 23,4 | 2,00 | 30,9 | 4,84 | 7,44 | 8,41 | 9,95 | 10,68 | 11,20 | 40,1 | 1 |
| | 0811 | 1 | 23,4 | 2,00 | 30,9 | 6,69 | 8,73 | 9,74 | 10,89 | 11,66 | 12,25 | 27,2 | 1 |
| | 0905 | 1 | 20,9 | 1,73 | 26,2 | 5,48 | 7,43 | 8,41 | 9,17 | 9,62 | 9,90 | $0,777 \cdot 10^{-1}$ | 1 |
| | 0906 | 1 | 20,9 | 1,73 | 26,2 | 5,57 | 7,70 | 8,50 | 9,53 | 9,98 | 10,34 | $0,757 \cdot 10^{-1}$ | 1 |
| | 0804 | 1 | 23,4 | 2,00 | 30,9 | 4,13 | 6,00 | 7,18 | 8,86 | 9,88 | 10,61 | $0,806 \cdot 10^{-1}$ | 1 |
| | 0805 | 1 | 23,4 | 2,00 | 30,9 | 4,73 | 6,70 | 7,78 | 9,44 | 10,52 | 11,38 | $0,931 \cdot 10^{-1}$ | 1 |
| | 0901 | 1 | 20,9 | 1,73 | 26,2 | 3,72 | 5,41 | 6,31 | 7,04 | 7,58 | 7,89 | $0,289 \cdot 10^{-3}$ | 1 |
| | 0801 | 1 | 23,4 | 2,00 | 30,9 | 2,63 | 5,00 | 6,00 | 7,47 | 8,37 | 9,04 | $0,300 \cdot 10^{-3}$ | 1 |
| | 0802 | 1 | 23,4 | 2,00 | 30,9 | 3,32 | 4,58 | 5,25 | 6,35 | 7,03 | 7,52 | $0,296 \cdot 10^{-3}$ | 1 |
| | 0707 | 2 | 44,5 | 2,88 | 34,9 | 12,35 | 17,08 | 19,66 | 22,61 | 23,43 | 23,35 | 107 | 1 |
| | 0708 | 2 | 44,5 | 2,88 | 34,9 | 10,31 | 16,90 | 19,56 | 21,93 | 22,27 | 22,10 | 117 | 1 |
| | 0709 | 2 | 44,5 | 2,88 | 34,9 | 12,54 | 17,59 | 19,84 | 21,75 | 21,63 | 21,07 | 124 | 1 |
| | 0710 | 2 | 44,5 | 2,88 | 34,9 | 9,62 | 14,52 | 16,38 | 18,29 | 19,22 | 19,73 | 23,4 | 1 |
| | 0711 | 2 | 44,5 | 2,88 | 34,9 | 12,35 | 16,82 | 18,68 | - | - | - | 25 | 1 |
| | 0712 | 2 | 44,5 | 2,88 | 34,9 | 10,32 | 15,39 | 17,28 | 19,10 | 19,61 | 20,03 | 23,9 | 1 |
| | 0602 | 2 | 46,4 | 3,03 | 34,4 | 10,55 | 15,20 | 17,10 | 19,19 | 20,03 | 20,46 | 30,3 | 1 |
| | 0701 | 2 | 44,5 | 2,88 | 34,9 | 9,21 | 14,69 | 17,49 | 20,65 | 22,24 | 23,01 | $0,823 \cdot 10^{-1}$ | 1 |
| | 0702 | 2 | 44,5 | 2,88 | 34,9 | 8,74 | 13,92 | 16,22 | 18,50 | 19,39 | 19,82 | $0,868 \cdot 10^{-1}$ | 1 |
| | 0703 | 2 | 44,5 | 2,88 | 34,9 | 10,05 | 14,73 | 16,46 | 18,14 | 18,89 | 19,39 | $0,860 \cdot 10^{-1}$ | 1 |
| | 0705 | 2 | 44,5 | 2,88 | 34,9 | 8,80 | 12,82 | 14,52 | 16,51 | 17,63 | 18,33 | $0,296 \cdot 10^{-3}$ | 1 |
| | 0706 | 2 | 44,5 | 2,88 | 34,9 | 9,09 | 12,90 | 14,53 | 16,46 | 17,63 | 18,40 | $0,294 \cdot 10^{-3}$ | 1 |
| | 0613 | 2 | 46,4 | 3,03 | 34,4 | 7,06 | 10,71 | 12,27 | 14,10 | 15,04 | 15,74 | $0,328 \cdot 10^{-3}$ | 1 |
| | 0614 | 2 | 46,4 | 3,03 | 34,4 | 7,77 | 10,99 | 12,47 | 14,28 | 15,37 | 16,01 | $0,297 \cdot 10^{-3}$ | 1 |

Table A7. continued

| type of steel | code* | mix | cube strength ($N/mm^2$) | splitting tensile strength ($N/mm^2$) | modulus of elasticity ($N/mm^2$) | bond stress $\tau$ for displacement $\delta =$ .. mm | | | | | | loading rate ($N/mm^2 \cdot ms$) | behaviour at failure** |
|---|---|---|---|---|---|---|---|---|---|---|---|---|---|
| | | | | | | 0,01 ($N/mm^2$) | 0,03 ($N/mm^2$) | 0,05 ($N/mm^2$) | 0,10 ($N/mm^2$) | 0,15 ($N/mm^2$) | 0,20 ($N/mm^2$) | | |
| | 1201 | 3 | 53,9 | 3,34 | 34,8 | 16,22 | 20,50 | 22,65 | 25,28 | 26,60 | 25,85 | 158 | 1 |
| | 1202 | 3 | 53,9 | 3,34 | 34,8 | 13,67 | 20,12 | 23,52 | 27,88 | 30,07 | 31,22 | 172 | 1 |
| | 1105 | 3 | 55,2 | 3,88 | 34,7 | 12,73 | 19,02 | 22,35 | 25,56 | 26,27 | 25,95 | 159 | 1 |
| | 1106* | 3 | 55,2 | 3,88 | 34,7 | 20,17 | 23,53 | 25,18 | 27,50 | 28,65 | 29,60 | 211 | 2 + 3 |
| | 1101 | 3 | 55,2 | 3,88 | 34,7 | 11,36 | 17,71 | 20,35 | 23,63 | 25,40 | 26,40 | 19,9 | 1 |
| | 1102 | 3 | 55,2 | 3,88 | 34,7 | 11,40 | 17,00 | 19,55 | 23,77 | 26,40 | - | 22,7 | 1 |
| | 1103 | 3 | 55,2 | 3,88 | 34,7 | 12,37 | 18,01 | 21,01 | 26,40 | - | - | 18,2 | 1 |
| | 1210 | 3 | 53,9 | 3,34 | 34,8 | 9,08 | 13,86 | 16,56 | 20,61 | 23,08 | 24,89 | $0,877 \cdot 10^{-1}$ | 3 |
| | 1211 | 3 | 53,9 | 3,88 | 34,7 | 10,23 | 15,52 | 18,72 | 24,06 | 27,59 | 30,54 | $0,872 \cdot 10^{-1}$ | 3 |
| | 1111 | 3 | 55,2 | 3,88 | 34,7 | 9,31 | 14,61 | 17,78 | 22,21 | 25,06 | 26,88 | $0,841 \cdot 10^{-1}$ | 3 |
| | 1112 | 3 | 55,2 | 3,88 | 34,7 | 10,66 | 16,24 | 19,83 | 25,07 | 28,13 | 29,73 | $0,852 \cdot 10^{-1}$ | 3 |
| | 1203 | 3 | 53,9 | 3,34 | 34,8 | 8,38 | 12,81 | 15,73 | 20,64 | 24,02 | - | $0,287 \cdot 10^{-3}$ | 3 |
| | 1205 | 3 | 53,9 | 3,34 | 34,8 | 8,05 | 12,95 | 15,82 | 20,27 | 23,09 | 24,88 | $0,289 \cdot 10^{-3}$ | 3 |
| | 1108 | 3 | 55,2 | 3,88 | 34,7 | 9,90 | 14,69 | 17,42 | 21,73 | 24,73 | 26,70 | $0,294 \cdot 10^{-3}$ | 3 |
| | 1110 | 3 | 55,2 | 3,88 | 34,7 | 8,86 | 13,59 | 16,19 | 20,24 | 22,79 | 24,65 | $0,297 \cdot 10^{-3}$ | 3 |
| plain steel, ø 10 | 0714 | 2 | 44,5 | 2,88 | 34,9 | 4,50 | 5,10 | | | | | 40 | 1 |
| | 0607 | 2 | 46,4 | 3,03 | 34,4 | 5,20 | 6,05 | | | | | $0,3 \cdot 10^{-3}$ | 1 |
| | 0608 | 2 | 46,4 | 3,03 | 34,4 | 4,35 | 4,90 | | | | | $0,3 \cdot 10^{-3}$ | 1 |
| | 1003 | 3 | 59,1 | 3,53 | 34,9 | 3,65 | 3,65 | | | | | 40 | 1 |
| | 1005 | 3 | 59,1 | 3,53 | 34,9 | 3,20 | 3,05 | | | | | 40 | 1 |
| | 1007 | 3 | 59,1 | 3,53 | 34,9 | 3,75 | 4,05 | | | | | $0,3 \cdot 10^{-3}$ | 1 |
| | 1008 | 3 | 59,1 | 3,53 | 34,9 | 3,50 | 3,65 | | | | | $0,3 \cdot 10^{-3}$ | 1 |
| pre-stress-ing strand, ø 9,6 | 1303 | 2 | 55,5 | 3,38 | - | 5,50 | 5,50 | 5,65 | 5,90 | 6,25 | 6,45 | 40 | 1 |
| | 1304 | 2 | 55,5 | 3,38 | - | 3,60 | 4,55 | 5,00 | 5,70 | 5,75 | 5,80 | 40 | 1 |
| | 1301 | 2 | 55,5 | 3,38 | - | 5,65 | 5,65 | 5,60 | 5,55 | 5,50 | 5,50 | $0,3 \cdot 10^{-3}$ | 1 |
| | 1302 | 2 | 55,5 | 3,38 | - | 5,50 | 6,00 | 5,95 | 6,00 | 6,15 | 6,20 | $0,3 \cdot 10^{-3}$ | 1 |

* key to code: first two digits indicate casting number, last two digits indicate specimen number

** failure behaviour: 1. slipping
2. splitting
3. tensile crack